

# 000 001 002 003 004 005 006 007 008 009 010 011 012 013 014 015 016 017 018 019 020 021 022 023 024 025 026 027 028 029 030 031 032 033 034 035 036 037 038 039 040 041 042 043 044 045 046 047 048 049 050 051 052 053 IDENTIFYING AND EVALUATING INACTIVE HEADS IN PRETRAINED LLMs

Anonymous authors

Paper under double-blind review

## ABSTRACT

Attention is foundational to large language models (LLMs), enabling different heads to have diverse focus on relevant input tokens. However, learned behaviors like attention sinks, where the first token receives the most attention despite limited semantic importance, suggest some heads may be inactive, and point to a significant source of computational redundancy. To analyze this phenomenon, we propose a taxonomy of 12 score functions that measure different ways a head can be inactive. Thresholding these scores allows us to analyze different sets of potentially inactive attention heads. We evaluate whether identified heads are inactive through model interventions, finding that more than 12% of attention heads are inactive on average, and can be ablated in specific contexts while maintaining MMLU accuracy to within 1% of the pretrained LLM. Across 3 model families, our score functions that measure the average norm of a head’s output consistently identify inactive heads that would not have been found by score functions that rely solely on attention weights. We establish that relying on a score function that measures a first token attention sink would underestimate the prevalence of inactive heads, failing to identify more than 7% of inactive heads on average. We also show how measuring score distributions can provide insights into attention behavior. For instance, we find evidence that finetuning causes little to no change in attention behavior, and that even within the same model family, large model scales present markedly different attention behaviors.

## 1 INTRODUCTION

Attention is a key component of the transformer architecture, which has led to breakthroughs in language modeling (Radford et al., 2019; Touvron et al., 2023; Dubey et al., 2024; OLMo et al., 2024; Yang et al., 2024). The attention mechanism allows tokens to incorporate information from relevant tokens, with multiple heads of attention capturing different types of relevance (Vaswani, 2017). But several works have found that attention can become “dormant” and concentrate on initial tokens, which are semantically irrelevant (Yu et al., 2024; Chen et al., 2025). The question we seek to answer is: How prevalent are inactive attention heads?

Depending on how one defines the word *inactive*, different answers are possible. Past work has focused exclusively on the attention weights (Guo et al., 2024a), labeling heads as “dormant” using a threshold-based score function. This is motivated by the idea that if a head attends primarily to the first token, and the first token has a near-zero value state, then the head output will be near-zero. However, this reasoning ignores other possibilities. Because an attention head’s output is a convex combination of value vectors, a head could attend to multiple tokens with near-zero value states to produce a near-zero output. In this work, we consider the many ways a head can be considered inactive, and produce a taxonomy of attention heads.

While classifying heads provides a useful taxonomy for understanding learned attention behaviors, identifying potentially inactive heads is not enough. Without zeroing out attention head outputs to erase their contribution to the hidden state, it is impossible to verify if identified heads are actually inactive. To address this, we perform model interventions while evaluating on the MMLU benchmark, and measure the effect of removing identified heads on model accuracy. Using 14 models across 3 model families, this experimental setup also allows us to analyze how attention head behaviors change as models scale and as models are finetuned. We make the following contributions:

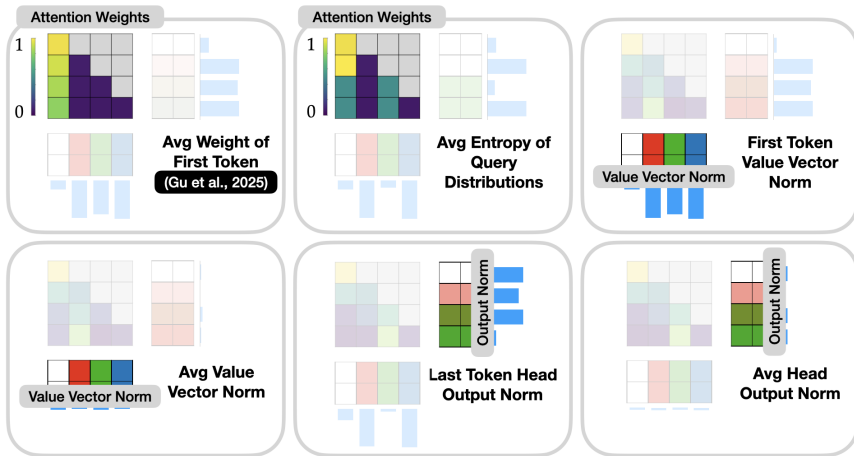


Figure 1: **The Inactive Head Taxonomy.** Our simple score functions measure all three components of attention: attention weights, value vectors, and head output vectors. In each cell, we give an example of the type of attention head that would be identified by each score function once scores are thresholded. For attention weights, the colorbar displays weights. For vectors, color represents direction, and length of the blue bar represents magnitude. For example, the Avg Weight of First Token score (Gu et al., 2025; Gu et al., 2024a) is calculated by computing average weight to the first token, and heads that exhibit high attention to the first token are identified if their their score exceeds a threshold. Value vectors and head outputs do not play a role, which we illustrate with a fade. Including normalized versions of these 6 score functions, there are 12 in total.

- We develop a taxonomy of 12 score functions that measure distinct properties of attention heads, and we threshold scores to classify attention heads, based on different definitions of *inactive*. We evaluate whether identified heads are truly inactive through model interventions which show that, on average, more than 12% of attention heads are inactive in pretrained LLMs we consider. Using prior characterizations of “dormant heads” would underestimate inactive heads, and fail to identify 7% of heads that are inactive.
- We find that, across model families and across model scale, inactive heads are consistently identified through the same score functions. In particular, measuring the average head output norm is most indicative. By finding a more model-agnostic score function, we provide evidence that inactive heads across transformer LLMs should be understood through head outputs rather than attention weights.
- We demonstrate that analyzing score distributions provides useful insights into attention: they reveal that finetuning induces minimal changes in attention behavior, and that scaling has little effect until models reach large sizes. Together, this suggests attention head behavior is more invariant to common training modifications than one might expect.

While our work has the potential to be used for efficient inference, our focus is strictly on understanding inactive attention heads. Specifically, how can we identify them and evaluate whether they are truly inactive?

## 2 BACKGROUND AND RELATED WORK

The idea that transformers may not be effectively utilizing all attention heads first came up in the context of machine translation. The work of Voita et al. (2019) and Michel et al. (2019) demonstrated that attention heads in transformer models could be removed with minor performance degradations. Methods for determining which heads can be removed have involved optimization of different kinds of objectives based on: stochastic gates (Voita et al., 2019), importance scores (Michel et al., 2019), iterative pruning (Behnke & Heafield, 2020), and subset pruning (Li et al., 2021). In this work, however, we do not use static pruning, where a head is permanently removed. Rather, our model intervention study (Section 4.3) is a form of dynamic pruning, where different heads are dropped

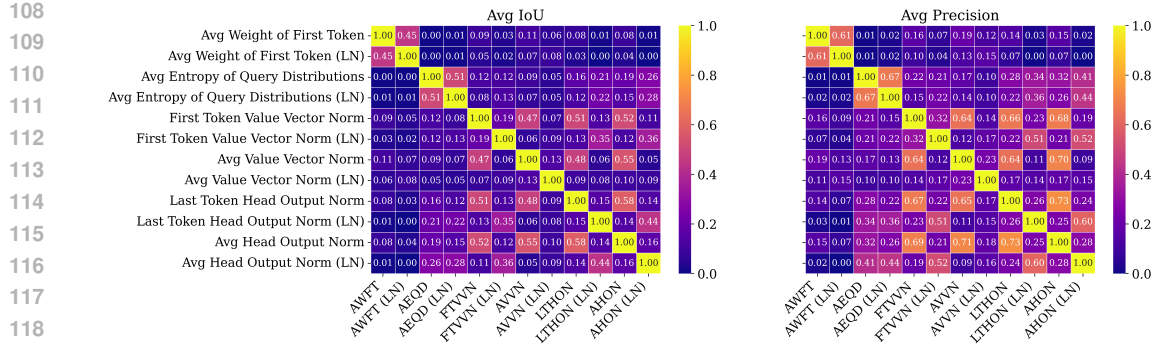


Figure 2: **Score functions identify different sets of heads.** Identifying different sets of heads ensures we capture a broad range of head characteristics, rather than focusing solely on the attention sink pattern of Avg Weight of First Token (Gu et al., 2025). Using 100 FineWeb-Edu training samples, we measure IoU of classifications between each score function on Llama-3.1-8B. We also measure Precision of one score function’s classifications relative to another’s, using the column score function as ground truth. Column score functions are abbreviated using the first letter of each word, and are in the same order as rows. For each score function, we dynamically choose thresholds such that  $\sim 10\%$  of heads are identified as potentially inactive. Even head scores normalized by scores of other heads in the layer, denoted by “(LN)”, do not show significant IoU or Precision with their unnormalized counterpart.

at every forward pass. Our objective is to measure how much head computation is wasted in each forward pass by inactive heads that can be zeroed out. We assume inactive heads are those that can be zeroed out, prior to concatenation and output projection of the multi-head attention mechanism.

**Multi-head attention.** The multi-head self-attention mechanism (Vaswani, 2017) allows multiple attention heads to operate in parallel, each focusing on different aspects of the input sequence. For an input of  $N$  tokens with dimensionality  $d_m$ , learned linear projections transform queries, keys, and values ( $\mathbf{Q}, \mathbf{K}, \mathbf{V} \in \mathbb{R}^{N \times d_m}$ ) into lower-dimensional representations:  $d_k$ -dimensional queries/keys and  $d_v$ -dimensional values, specific to each of the  $h$  heads. The self-attention operation within each head computes attention weights, defined as  $\mathbf{A} = \text{softmax}(\frac{\mathbf{Q}\mathbf{K}^\top}{\sqrt{d_k}})$ , where  $\mathbf{A} \in [0, 1]^{N \times N}$  and each row sums to 1, which are then applied to the value vectors. Another way to view the output of the  $i^{\text{th}}$  attention head  $\mathbf{head}^i \in \mathbb{R}^{N \times d_v}$  is that, for every position in the sequence, we compute a convex combination of value vectors, weighted by the corresponding row of  $\mathbf{A}$ . The outputs of all heads are concatenated and passed through a final linear projection to produce the module’s output. The attention weights,  $\mathbf{A}$ , are one of the few features we can visualize to get a sense of how pretrained LLMs work. For a token sequence, high attention weights (close to 1) reveal which tokens are considered most relevant. Thus, it is surprising that attention can concentrate on initial tokens, called “attention sinks”, as shown in App. Figure 19.

**Attention sinks.** An attention sink or sink token is a token that, despite limited semantic importance, disproportionately receives high attention weight from other tokens in a sequence. They tend to occur either at the first position of the input sequence (Xiao et al., 2024; Guo et al., 2024a), at certain word tokens (e.g., “and” and “of”), or delimiter tokens (Sun et al., 2024; Yu et al., 2024). The first token can be an attention sink even when it is not a BOS token (Xiao et al., 2024; Gu et al., 2025). To understand the prevalence of attention heads with sinks, Gu et al. (2025) propose to measure the average weight assigned to the first token and check if it exceeds a threshold  $\tau$ :  $\frac{1}{N} \sum_{i=0}^{N-1} \mathbf{A}_{i,0} > \tau$ . In our work, we refer to this metric as “Avg Weight of First Token” and use it as a starting point, but ultimately find that different threshold-based score functions are needed for identifying inactive heads in model families outside of Llama (Dubey et al., 2024) and GPT-2 (Radford et al., 2019).

As can be seen in App. Figure 19, attention sinks also exhibit value-state drains (Guo et al., 2024b; Gu et al., 2025; Kobayashi et al., 2020), where the norm of the value state is near zero. Note that if the sink token’s value state is zero but the attention weight to the sink token is one, the output of

162  
 163 Table 1: **Equations for Inactive Head Taxonomy.** We define how each score function is used to  
 164 identify inactive heads with a threshold-based rule. Sample attention heads are in Appendix A.3  
 165 Figure 7. We sweep a range of thresholds  $\tau$  for each function.

Score Function	Definition
Avg Weight of First Token (AWFT)	$\frac{1}{N} \sum_{i=0}^{N-1} \mathbf{A}_{i,0} > \tau$
Avg Entropy of Query Distributions (AEQD)	$\frac{1}{N} \sum_{i=0}^{N-1} \text{Ent}(\mathbf{A}_{i,:}) < \tau$
First Token Value Vector Norm (FTVVN)	$\ \mathbf{V}_{0,:}\ _2 < \tau$
Avg Value Vector Norm (AVVN)	$\frac{1}{N} \sum_{i=0}^{N-1} \ \mathbf{V}_{i,:}\ _2 < \tau$
Last Token Head Output Norm (LTHON)	$\ \text{head}_{N-1,:}^i\ _2 < \tau$
Avg Head Output Norm (AHON)	$\frac{1}{N} \sum_{i=0}^{N-1} \ \text{head}_{i,:}^i\ _2 < \tau$

177  
 178 this head (prior to the output projection) is zero, leading Guo et al. (2024a) to call this a dormant  
 179 attention head.  
 180

181 **Dormant attention.** Guo et al. (2024a) propose the idea that attention heads can be either active or  
 182 dormant. They perform a model intervention study on 3 attention heads of Llama-2-7B Base, where  
 183 a specific attention head output is zeroed out, and the difference in loss as a result of the intervention  
 184 is measured. They find that the difference in loss can depend on whether input text is from Wikipedia  
 185 or GitHub; a head that is dormant on Wikipedia samples does not change the loss when the head  
 186 output is zeroed. In our work, we go beyond analyzing one attention head at a time and propose to  
 187 zero out all “dormant heads” while evaluating models on a real-world benchmark task. If “dormant  
 188 heads” are truly inactive, then zeroing them out should have little effect on model performance. We  
 189 also propose new score functions that measure different definitions of *inactive*. Unlike Guo et al.  
 190 (2024a) and Gu et al. (2025) who measure only attention weights, our score functions also consider  
 191 value vectors and head outputs. By considering the range of ways a head can be inactive, we present  
 192 a more accurate picture of inactive attention heads in pretrained models. A better understanding  
 193 of inactive attention heads has the potential to be used for efficiency (Li et al., 2021), KV cache  
 194 reduction (Liu et al., 2023), and compression (Ge et al., 2024).

### 195 3 THE INACTIVE HEAD TAXONOMY

196 We outline a number of simple score functions, each capturing different ways a head could be  
 197 considered inactive. Each score function assigns a score to every attention head in a transformer  
 198 LLM. By thresholding the scores, we classify and study different sets of heads. We summarize each  
 199 score function in Table 1. We use the  $\ell_2$ -norm wherever applicable.  
 200

201 **Attention patterns.** An attention head could appear inactive due to the patterns in its attention  
 202 weights. Both overly focused and overly diffuse attention can be considered “inactive,” depending  
 203 on the input. Prior work has recognized the case where attention can concentrate on a single token  
 204 (Gu et al., 2025; Guo et al., 2024a), where attention is distributed too little, and quantified it by  
 205 calculating the Average Weight of the First Token (AWFT). However, this does not capture the case  
 206 where there are multiple sink tokens (See App. Figure 19). To measure when attention concentrates  
 207 on a few tokens, we choose to measure the Entropy of each Query’s Distribution over keys, averaged  
 208 over all queries. Calculating this amounts to measuring entropy of each row of the attention weights,  
 209 then taking an average. If average entropy of the head is low, it implies attention concentrates on  
 210 few tokens. If a head’s average entropy is under a threshold  $\tau$ , we can classify it as potentially  
 211 inactive. The smaller we make  $\tau$ , the more strict we are in classifying heads that exhibit this pattern.  
 212 Changing the direction of the inequality in Avg Entropy of Query Distributions could capture cases  
 213 where attention is too uniform (*i.e.*, too much attention to all keys), but we chose not to consider this  
 214 case because heads in early layers tend to exhibit this pattern, and early layers tend to be important  
 215 (Sun et al., 2025).

216 **Value vectors.** An attention head could *appear* active with its attention patterns, but could be  
 217 inactive if all the value vectors are near-zero. To measure this, we compute Avg Value Vector Norm:  
 218 the average  $\ell_2$ -norm of value vectors in the head. It is also possible that while attention patterns may  
 219 not primarily concentrate on the first token, some tokens could still use the first token as a “value-  
 220 state drain” (Guo et al., 2024a). To capture heads that do this, we compute the First Token Value  
 221 Vector Norm, *i.e.*, the  $\ell_2$ -norm of the value vector corresponding to the first position. As with other  
 222 score functions, we consider normalizing by the average score of other heads in the layer.

223 **Head outputs.** Finally, an attention head could be inactive if its output is small. This key assumption  
 224 is most closely captured by the score functions that measure the head output: when a head  
 225 produces small outputs, its contribution to the residual stream will be minimal, and these heads can  
 226 be zeroed with little to no accuracy drop. Because multiple choice (MC) benchmark evaluations re-  
 227 trieve the probability assigned by the model to the correct answer from the probability distribution of  
 228 the last position, we also propose to measure the Last Token Head Output Norm. To capture cases  
 229 where most positions have head outputs that are small, we measure the Avg Head Output Norm.  
 230 More information on why we do not use the circuit-based definition of a head output can be found  
 231 in Appendix A.1.

232 **Normalization.** We classify heads using the score functions in Table 1, but we also consider nor-  
 233 malization by the score of other heads in the same layer. Abusing terminology, we refer to this as  
 234 layer normalization, or “(LN)” throughout. As an example, the Avg Head Output Norm (AHON)  
 235 score function for the  $i^{\text{th}}$  attention head in a layer is computed as follows:  $\text{AvgNorm}(\text{head}^i)$ , where  
 236  $\text{AvgNorm}(T) = \frac{1}{N} \sum_{i=0}^N \|T_{i,:}\|_2$  computes the average  $\ell_2$ -norm of the rows of input matrix  $T$  and  
 237 where  $\text{head}^i \in \mathbb{R}^{N \times d_v}$  is the head output. Then, the normalized version, Avg Head Output Norm  
 238 (LN), is simply normalized by the average AHON score of heads in the same layer:

$$\frac{\text{AvgNorm}(\text{head}^i)}{\frac{1}{N_{\text{layer}}} \sum_{j=0}^{N_{\text{layer}}} \text{AvgNorm}(\text{head}^j)} \quad (1)$$

244 Thresholding the score of Equation (1) whenever it is  $< \tau$  controls how strictly we classify a head  
 245 as inactive. For example, when  $\tau = 0.1$ , heads with output norms less than 10% of the layer average  
 246 are considered inactive. Code implementations are provided in Appendix A.13.

## 4 EXPERIMENTS

251 First, we study which score function is best at identifying inactive heads. Then, we use head scores  
 252 to study how attention behaviors change as models scale and are finetuned.

### 4.1 SETUP

256 We download 14 pretrained models using Hugging Face transformers (Wolf et al., 2020):  
 257 Llama-3.1-8B, Llama-3.1-8B-Instruct (Dubey et al., 2024), Llama-3.2-3B, Llama-3.2-3B-Instruct  
 258 (Meta, 2024), OLMo-2-1124-7B, OLMo-2-1124-7B-SFT, OLMo-2-1124-7B-DPO, OLMo-2-1124-  
 259 7B-Instruct (OLMo et al., 2024), Qwen2.5-0.5B, Qwen2.5-1.5B, Qwen2.5-3B, Qwen2.5-7B,  
 260 Qwen2.5-7B-Instruct, and Qwen2.5-14B (Yang et al., 2024). We refer to models from the same  
 261 organization as belonging to the same “model family.” We evaluate models on MMLU (Hendrycks  
 262 et al., 2021) (5-shot) in our model intervention experiments. For datasets that do not use an LLM-  
 263 as-a-Judge, MMLU is the multiple-choice (MC) benchmark with the highest Spearman correlation  
 264 with ChatBot Arena (Li et al., 2023; Chiang et al., 2024), and thus makes it the most ap-  
 265 propriate choice for aligning with real-world chatbot preferences while keeping evaluation consis-  
 266 tent and tractable. Additional results on PIQA (0-shot) (Bisk et al., 2020) and WinoGrande (5-  
 267 shot) (Sakaguchi et al., 2021) can be found in Appendix A.4. All evaluations are performed using  
 268 1m-evaluation-harness (Gao et al., 2024). We also use FineWeb-Edu (Lozhkov et al., 2024),  
 269 which is a pretraining dataset of educational webpages. We randomly truncate FineWeb-Edu train-  
 270 ing sequences to between 10 and 3000 tokens to exhibit a variety of sequence lengths. Additional  
 271 model and dataset details are in Appendix A.14.

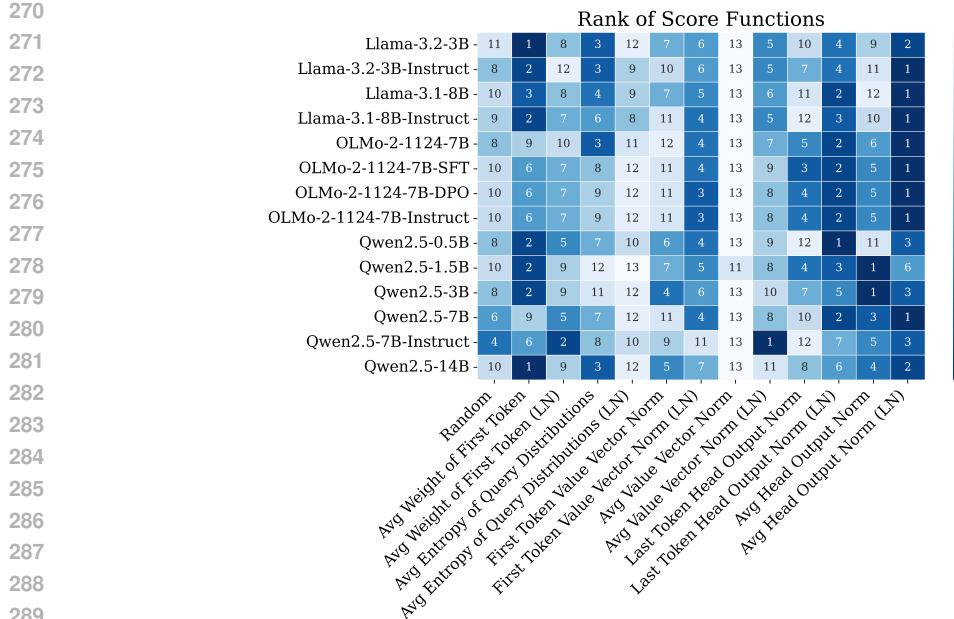


Figure 3: **Measuring Avg Head Output Norm is best at identifying inactive heads for most models.** For every model, we rank the 12 scoring functions by normalized AUC, which captures their ability to select inactive heads. Avg Head Output Norm (LN) ranks 1<sup>st</sup> for 8 out of 14 models, and ranks in top-3 for 13 out of 14 models. Top scoring functions are consistent across model families.

**Metrics and Thresholds.** In a transformer with  $N_{\text{heads}}$  attention heads per  $N_{\text{layers}}$  layers, and a dataset  $\mathcal{D}$  of token sequences, a forward pass on input sequence  $x \in \mathcal{D}$  will produce attention weights, value states, and head outputs for every head. We measure these components, and assign a score to every head, arranged in a matrix  $\mathbf{S} \in \mathbb{R}^{N_{\text{heads}} \times N_{\text{layers}}}$ . Thresholding  $\mathbf{S}$  results in a boolean matrix  $\mathbf{B}$  of the same size. In our model intervention experiments, a different boolean matrix is constructed for every new forward pass and “% of Model Heads Zeroed” refers to the percent of True values in  $\mathbf{B}$ , averaged over all token sequences in  $\mathcal{D}$ . The proportion of heads each score function identifies as inactive can be controlled by the threshold  $\tau$ , which we vary for each function. The thresholds for each score function are chosen by measuring head scores across MMLU inputs, constructing the CDF of scores, and calculating the  $p$ -th quantile<sup>1</sup> for  $p \in [0, 5, 10, 15, 20, 25, 30]$ . This way, we can estimate the proportion of heads that will be selected for each threshold, allowing us to focus on zeroing out at most 30% of heads. All score distributions are in App. Figure 16.

## 4.2 SCORE FUNCTIONS IDENTIFY DIFFERENT SETS OF HEADS

To ensure that each score function measures a different aspect of attention heads, we measure the agreement between predictions (post-thresholding) using IoU. We also measure precision, taking one of the score functions as ground truth. We use Llama-3.1-8B and 100 FineWeb-Edu sequences to collect scores, and we threshold them dynamically to make predictions. In Figure 2, we see that the max IoU is 0.58, while the max Precision is 0.73. This suggests no score function is effectively the same as another. High agreement tends to occur between unnormalized and normalized pairs of score functions (*i.e.*, AWFT and AWFT (LN)), but not always. For example, Last Token Head Output Norm has an IoU of 0.58 with Average Head Output Norm. In a similar vein, First Token Value Vector Norm has an IoU of 0.47 with Average Value Vector Norm. This effect may occur because the presence of small-magnitude vectors drives down the overall average magnitude. The score function that best predicts the same heads as AWFT is AWFT (LN) with a precision of 0.61. Notably, normalizing by the average score of other heads in the layer significantly reorders heads. All other score functions have Precision under 0.19 with AWFT. Because each scoring function

<sup>1</sup>In the case of Avg Weight of the First Token, we calculate the  $(1 - p)$ -th quantile because the threshold inequality reversed.

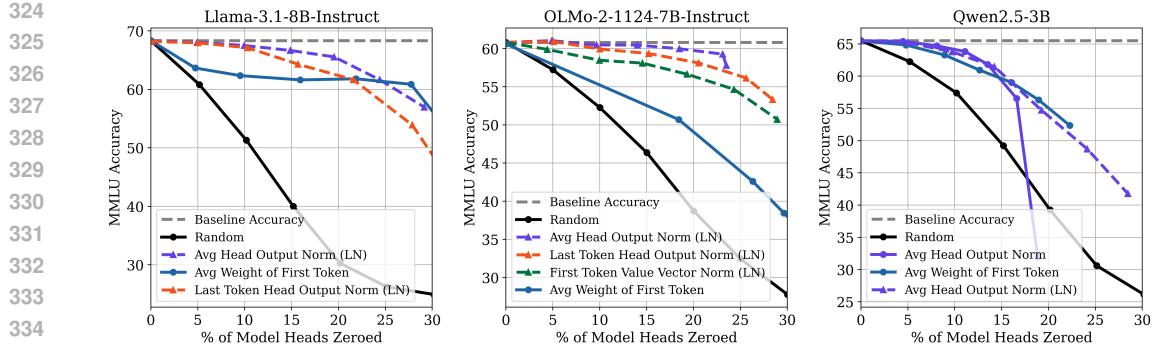


Figure 4: **Inactive heads can be identified and zeroed with minor performance degradation.** For each model, we plot the top-3 scoring functions. Average Weight of First Token is not in the top-3 for OLMo-2-1124-7B-Instruct, but we include it for comparison to prior work. The gray dotted line represents baseline accuracy of the pretrained model. The black line represents zeroing out heads uniformly at random. The Avg Head Output Norm (LN) scoring function is best at identifying the most heads, that when zeroed, maintain accuracy. Complete results for all models and score functions can be found in App. Figure 9.

Table 2: **On average, more than 12% of attention heads can be zeroed while keeping average accuracy within 1% of the original model.** For every model, we calculate the highest percentage of heads that can be zeroed using Average Weight of First Token (AWFT), and compare to our score functions (*i.e.*, all score functions excluding AWFT). Higher is better. The overall best score function is also shown. Our score functions only improve or are within less than 0.3% of AWFT. We are able to identify and verify more inactive heads than previously possible with AWFT. Specifically, using AWFT would classify less than 5% of heads as inactive, which misses 7% of heads, on average.

Model	% of Heads Zeroed		Best Score Function
	AWFT	Ours	
Llama-3.2-3B	8.34	8.05 (-0.29)	Avg Weight of First Token
Llama-3.2-3B-Instruct	6.87	13.04 (+6.17)	Avg Head Output Norm (LN)
Llama-3.1-8B	8.56	17.11 (+8.55)	Avg Head Output Norm (LN)
Llama-3.1-8B-Instruct	1.01	10.97 (+9.95)	Avg Head Output Norm (LN)
OLMo-2-1124-7B	0.42	8.34 (+7.93)	Avg Head Output Norm (LN)
OLMo-2-1124-7B-SFT	1.70	18.95 (+17.25)	Avg Head Output Norm (LN)
OLMo-2-1124-7B-DPO	2.14	20.60 (+18.46)	Avg Head Output Norm (LN)
OLMo-2-1124-7B-Instruct	1.46	19.54 (+18.07)	Avg Head Output Norm (LN)
Qwen2.5-0.5B	7.43	14.42 (+6.99)	Last Token Head Output Norm (LN)
Qwen2.5-1.5B	7.55	7.49 (-0.07)	Avg Weight of First Token
Qwen2.5-3B	5.67	8.78 (+3.11)	Avg Head Output Norm
Qwen2.5-7B	1.25	7.54 (+6.29)	Avg Head Output Norm (LN)
Qwen2.5-7B-Instruct	1.13	5.76 (+4.63)	Avg Value Vector Norm (LN)
Qwen2.5-14B	11.04	9.88 (-1.17)	Avg Weight of First Token
Average	4.61	12.18 (+7.56)	-

identifies a distinct subset of heads, we can verify their predictions with confidence that they capture different underlying properties.

#### 4.3 VERIFYING INACTIVE HEADS THROUGH MODEL INTERVENTIONS

To verify inactive attention heads, we conduct model interventions by zeroing out the outputs of identified heads from each score function, and measuring the resulting impact on model accuracy. For every model, we also compare to a random baseline where attention heads are zeroed uniformly

378 at random. An effective inactive head score function should identify a substantial fraction of heads  
 379 that can be zeroed out without compromising the performance of the pretrained model. What score  
 380 function is best at identifying inactive attention heads?

381 In Figure 4, we measure how MMLU accuracy changes as we zero out heads selected by different  
 382 score functions. For brevity, we present one model from each model family: Llama-3.1-8B-Instruct,  
 383 OLMo-2-1124-7B-Instruct, and Qwen2.5-3B. To do this, we vary the threshold of each score func-  
 384 tion such that identified heads are at most 30% of the model’s heads. We plot the top-3 score  
 385 functions for every model in Figure 4, but complete results for all models and score functions can  
 386 be found in App. Figure 9. In Table 2, we quantify the percent of heads that can be zeroed while  
 387 keeping accuracy to within 1% of baseline. We find that, for 8 out of 14 models, the Avg Head  
 388 Output Norm (LN) score function is best at identifying the most attention heads that when zeroed,  
 389 maintain accuracy to within 1% of baseline. For 13 out of 14 models, AHON (LN) ranks in the  
 390 top-3 scoring functions. Avg Weight of First Token underestimates the number of inactive heads.

391 The fact that a single, simple threshold-based function like Avg Head Output (LN) can identify the  
 392 most inactive heads for multiple models, suggests that looking at attention weights is a misleading  
 393 signal. While heads with attention sink patterns seem to occur in all models we consider (See  
 394 App Figure 19), our results suggest these patterns are not solely indicative of inactivity. Moreover,  
 395 our results confirm that while attention head patterns may appear “dormant” (Guo et al., 2024a),  
 396 their outputs are not. Removing attention heads using Avg Weight of First Token as the score is  
 397 particularly ineffective for OLMo-2 models. While it is appealing to look only at attention patterns  
 398 as a consistent feature across models of varying organizations and architectures, it appears that small  
 399 head outputs are consistently more indicative of inactivity.

400 Despite looking for negligible head outputs, the complexity and non-linearity of LLMs make it  
 401 difficult to know whether heads with “small” outputs can be zeroed while maintaining accuracy. To  
 402 the best of our knowledge, we are the first to systematically evaluate the degree of head inactivity  
 403 and investigate whether these heads are unnecessary. **Takeaway:** Inactive attention heads are best  
 404 identified by measuring Avg Head Output Norm (LN). Measuring attention weight patterns like Avg  
 405 Weight of First Token are not model-agnostic.

406  
 407 **Ranking Score Functions.** Each of 12 score functions use a different set of 7 thresholds. Accu-  
 408 racy curves that terminate at different x-axis values make it difficult to assess which method is best.  
 409 So, we choose to measure performance by Area Under the Curve (AUC) normalized by the x-axis  
 410 span of each accuracy curve. For every model, the ranking of each score function is displayed in  
 411 Figure 3. Notably, Avg Head Output Norm and its normalized version are more model-agnostic,  
 412 ranking 1<sup>st</sup> for 10 out of 14 models. In contrast, Avg Weight of First Token ranks 1<sup>st</sup> for only  
 413 Llama-3.2-3B and Qwen2.5-14B, and performs most poorly for the OLMo-2 family of models.

#### 414 4.4 SCORE DISTRIBUTIONS FOR STUDYING ATTENTION BEHAVIORS

415 As described in Section 3, each score quantifies a characteristic about an attention head: how much  
 416 attention is paid to the first token, how small is the first value vector, how small is the average head  
 417 output, etc. Analyzing the scores of heads can give us a broad idea of attention head behavior.  
 418 Every model and score function combination produces a distribution of scores. By measuring the  
 419 similarity of these score distributions, we can determine whether attention behavior is similar or  
 420 different. With the exception of the AWFT score function, most score distributions have similar  
 421 modes (See App. Figure 16). Thus, we chose the Wasserstein distance to measure similarity between  
 422 head score distributions. In Figure 5, we see that AWFT score distributions are similar within a  
 423 model family, illustrated by a dark block diagonal pattern. The only outlier is Qwen2.5-14B, which  
 424 has distributions more similar to Llama models than Qwen2.5 models. For AHON (LN) score  
 425 distributions, Llama and OLMo-2 models are more similar to each other than to Qwen2.5 models.

426 We use the Qwen2.5 models (Yang et al., 2024) to understand how model scale affects attention  
 427 head behaviors. There are 5 model types ranging from 0.5B parameters to 14B parameters, but  
 428 while the models share the same pre-training data, the exact number of training tokens each model  
 429 was exposed to is not publicly documented. Assuming model scale is the only variable, it appears  
 430 that model scale impacts attention head behaviors. As Qwen2.5 models grow in size, they are quite  
 431 similar to one another, until the 14B scale. For example, on most score functions, Wasserstein

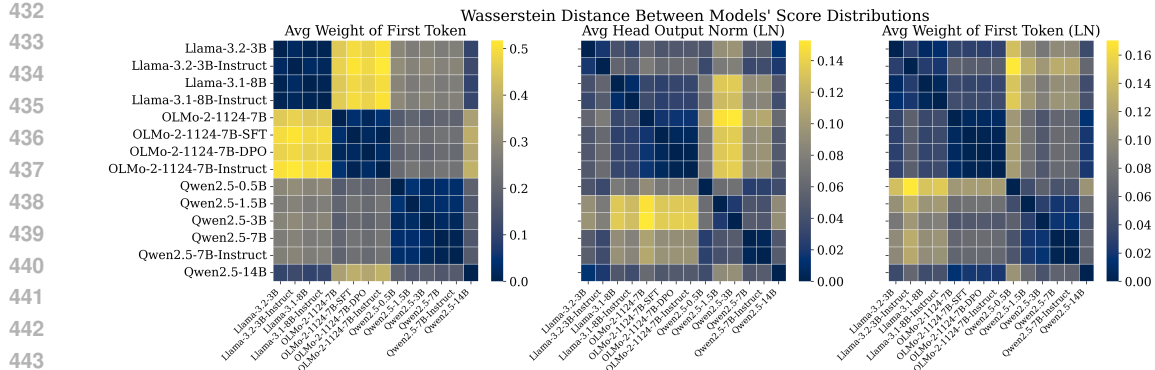


Figure 5: **Head score distributions can be similar within a model family.** Smaller Wasserstein distances indicate similar score distributions. Full results for all 13 scoring functions can be found in App. Figure 17.

distance is near-zero, indicated by a clear dark region that corresponds to inter-model similarity. But at the 14B scale, there appears to be only 2 score function distribution where Qwen2.5-14B is similar to other models in the Qwen2.5 family: Avg Value Vector Norm and its layer normalized version. This may suggest that larger models learn to specialize their heads in different ways. The similarity of score distributions between the Llama-3 models we consider may have more to do with their training objective as opposed to training data. In particular, because Llama-3.2 was created from pruning Llama-3.1-8B, then performing knowledge distillation, these models are *trained* to be similar (Meta, 2024).

To study finetuning, we primarily rely on the OLMo-2 models which have checkpoints after SFT, after DPO (Rafailov et al., 2023), and after RLHF (Lambert et al., 2024). We also have the Instruct models corresponding to the Llama-3.2-3B, Llama-3.1-8B, and Qwen2.5-7B base models. Figures 5 and 17 illustrate that all finetuning strategies we consider (SFT, DPO, RLHF) have nearly no effect on score distributions, suggesting little change in attention behaviors. Across all score functions, finetuned models have the smallest Wasserstein distances with their base model. In the case of all the OLMo-2 models, the Wasserstein distances of their score distributions are more similar to each other than any other model. These results indicate that finetuning primarily preserves the underlying attention head behaviors of the base model.

## 5 CONCLUSION

Understanding when attention heads are inactive requires looking beyond attention weights. Simple score functions, based on previously ignored components like value vectors and head outputs, can capture a wider array of inactivity. By assigning different scores to every head in a transformer LLM, we can classify different subsets of attention heads as inactive using a threshold. While there is some overlap in the subsets of inactive heads we classify using different scoring functions, we find that most scoring functions capture diverse characteristics. By zeroing out identified inactive heads during MMLU evaluations, we find that more than 12% of heads can be zeroed out while maintaining accuracy to within 1% of the baseline model, on average. Using a score function based on a first token attention sink would classify less than 5% of heads as inactive on average, which underestimates the true prevalence of inactive heads. For the majority of models we consider, the score function that measures average head output norm produces the best signal for identifying inactive heads across model families. While attention sinks and sink tokens are almost synonymous with an inactive head, our work demonstrates that there are other sets of heads that are more inactive, and that we can identify them in a more model-agnostic way. Additionally, we show how measuring score distributions can be informative: we use them to explore how finetuning causes little to no change to attention behavior, and how model scale does very little to attention behavior until very large scale. Future work could consider how the MLP module, which proceeds the attention module, could be inactive per-token if converged to an optimal hidden state.

486 REFERENCES  
487

488 Joshua Ainslie, James Lee-Thorp, Michiel de Jong, Yury Zemlyanskiy, Federico Lebron, and Sumit  
489 Sanghai. GQA: Training generalized multi-query transformer models from multi-head check-  
490 points. In *The 2023 Conference on Empirical Methods in Natural Language Processing*, 2023.  
491 URL <https://openreview.net/forum?id=hmOwOZWzYE>.

492 Maximiliana Behnke and Kenneth Heafield. Losing heads in the lottery: Pruning transformer. In  
493 *The 2020 Conference on Empirical Methods in Natural Language Processing*, pp. 2664–2674.  
494 Association for Computational Linguistics (ACL), 2020.  
495

496 Yonatan Bisk, Rowan Zellers, Jianfeng Gao, Yejin Choi, et al. Piqa: Reasoning about physical com-  
497 monsense in natural language. In *Proceedings of the AAAI conference on artificial intelligence*,  
498 volume 34, pp. 7432–7439, 2020.

499 Liang Chen, Haozhe Zhao, Tianyu Liu, Shuai Bai, Junyang Lin, Chang Zhou, and Baobao Chang.  
500 An image is worth 1/2 tokens after layer 2: Plug-and-play inference acceleration for large vision-  
501 language models. In *European Conference on Computer Vision*, pp. 19–35. Springer, 2025.  
502

503 Wei-Lin Chiang, Lianmin Zheng, Ying Sheng, Anastasios Nikolas Angelopoulos, Tianle Li,  
504 Dacheng Li, Hao Zhang, Banghua Zhu, Michael Jordan, Joseph E. Gonzalez, and Ion Stoica.  
505 Chatbot arena: An open platform for evaluating llms by human preference, 2024.

506 Abhimanyu Dubey, Abhinav Jauhri, Abhinav Pandey, Abhishek Kadian, Ahmad Al-Dahle, Aiesha  
507 Letman, Akhil Mathur, Alan Schelten, Amy Yang, Angela Fan, et al. The llama 3 herd of models.  
508 *arXiv preprint arXiv:2407.21783*, 2024.  
509

510 Nelson Elhage, Neel Nanda, Catherine Olsson, Tom Henighan, Nicholas Joseph, Ben Mann,  
511 Amanda Askell, Yuntao Bai, Anna Chen, Tom Conerly, Nova DasSarma, Dawn Drain, Deep  
512 Ganguli, Zac Hatfield-Dodds, Danny Hernandez, Andy Jones, Jackson Kernion, Liane Lovitt,  
513 Kamal Ndousse, Dario Amodei, Tom Brown, Jack Clark, Jared Kaplan, Sam McCandlish, and  
514 Chris Olah. A mathematical framework for transformer circuits. *Transformer Circuits Thread*,  
515 2021. <https://transformer-circuits.pub/2021/framework/index.html>.

516 Leo Gao, Jonathan Tow, Baber Abbasi, Stella Biderman, Sid Black, Anthony DiPofi, Charles Fos-  
517 ter, Laurence Golding, Jeffrey Hsu, Alain Le Noac'h, Haonan Li, Kyle McDonell, Niklas Muen-  
518 nighoff, Chris Ociepa, Jason Phang, Laria Reynolds, Hailey Schoelkopf, Aviya Skowron, Lin-  
519 tang Sutawika, Eric Tang, Anish Thite, Ben Wang, Kevin Wang, and Andy Zou. A framework  
520 for few-shot language model evaluation, 07 2024. URL <https://zenodo.org/records/12608602>.  
521

522 Suyu Ge, Yunan Zhang, Liyuan Liu, Minjia Zhang, Jiawei Han, and Jianfeng Gao. Model tells  
523 you what to discard: Adaptive KV cache compression for LLMs. In *The Twelfth International*  
524 *Conference on Learning Representations*, 2024. URL <https://openreview.net/forum?id=uNrFpDPMyo>.  
525

526 Xiangming Gu, Tianyu Pang, Chao Du, Qian Liu, Fengzhuo Zhang, Cunxiao Du, Ye Wang, and  
527 Min Lin. When attention sink emerges in language models: An empirical view. In *The Thirteenth*  
528 *International Conference on Learning Representations*, 2025. URL <https://openreview.net/forum?id=78Nn4QJTEN>.  
529

530 Tianyu Guo, Druv Pai, Yu Bai, Jiantao Jiao, Michael I. Jordan, and Song Mei. Active-dormant  
531 attention heads: Mechanistically demystifying extreme-token phenomena in llms, 2024a. URL  
532 <https://arxiv.org/abs/2410.13835>.  
533

534 Zhiyu Guo, Hidetaka Kamigaito, and Taro Watanabe. Attention score is not all you need for to-  
535 ken importance indicator in KV cache reduction: Value also matters. In Yaser Al-Onaizan,  
536 Mohit Bansal, and Yun-Nung Chen (eds.), *Proceedings of the 2024 Conference on Empirical*  
537 *Methods in Natural Language Processing*, pp. 21158–21166, Miami, Florida, USA, November  
538 2024b. Association for Computational Linguistics. doi: 10.18653/v1/2024.emnlp-main.1178.  
539 URL <https://aclanthology.org/2024.emnlp-main.1178/>.

540 Dan Hendrycks, Collin Burns, Steven Basart, Andy Zou, Mantas Mazeika, Dawn Song, and Jacob  
 541 Steinhardt. Measuring massive multitask language understanding. *Proceedings of the Interna-*  
 542 *tional Conference on Learning Representations (ICLR)*, 2021.

543

544 Goro Kobayashi, Tatsuki Kuribayashi, Sho Yokoi, and Kentaro Inui. Attention is not only a weight:  
 545 Analyzing transformers with vector norms. In Bonnie Webber, Trevor Cohn, Yulan He, and  
 546 Yang Liu (eds.), *Proceedings of the 2020 Conference on Empirical Methods in Natural Language*  
 547 *Processing (EMNLP)*, pp. 7057–7075, Online, November 2020. Association for Computational  
 548 Linguistics. doi: 10.18653/v1/2020.emnlp-main.574. URL <https://aclanthology.org/2020.emnlp-main.574/>.

549

550 Nathan Lambert, Jacob Morrison, Valentina Pyatkin, Shengyi Huang, Hamish Ivison, Faeze Brah-  
 551 man, Lester James V Miranda, Alisa Liu, Nouha Dziri, Shane Lyu, et al. Tulu 3: Pushing frontiers  
 552 in open language model post-training. *arXiv preprint arXiv:2411.15124*, 2024.

553

554 Jiaoda Li, Ryan Cotterell, and Mrinmaya Sachan. Differentiable subset pruning of transformer  
 555 heads. *Transactions of the Association for Computational Linguistics*, 9:1442–1459, 2021.

556

557 Xuechen Li, Tianyi Zhang, Yann Dubois, Rohan Taori, Ishaan Gulrajani, Carlos Guestrin, Percy  
 558 Liang, and Tatsunori B. Hashimoto. Alpacaeval: An automatic evaluator of instruction-following  
 559 models. [https://github.com/tatsu-lab/alpaca\\_eval](https://github.com/tatsu-lab/alpaca_eval), 5 2023.

560

561 Ji Lin, Yongming Rao, Jiwen Lu, and Jie Zhou. Runtime neural pruning. *Advances in neural*  
 562 *information processing systems*, 30, 2017.

563

564 Zichang Liu, Aditya Desai, Fangshuo Liao, Weitao Wang, Victor Xie, Zhaozhuo Xu, Anastasios  
 565 Kyrillidis, and Anshumali Shrivastava. Scissorhands: Exploiting the persistence of importance  
 566 hypothesis for llm kv cache compression at test time. *Advances in Neural Information Processing*  
 567 *Systems*, 36:52342–52364, 2023.

568

569 Anton Lozhkov, Loubna Ben Allal, Leandro von Werra, and Thomas Wolf. Fineweb-edu: the finest  
 570 collection of educational content, 2024. URL <https://huggingface.co/datasets/HuggingFaceFW/fineweb-edu>.

571

572 Meta. Llama 3.2: Revolutionizing edge ai and vision with open, cus-  
 573 tomizable models, Sep 2024. URL <https://ai.meta.com/blog/llama-3-2-connect-2024-vision-edge-mobile-devices/>.

574

575 Paul Michel, Omer Levy, and Graham Neubig. Are sixteen heads really better than one? *Advances*  
 576 *in neural information processing systems*, 32, 2019.

577

578 Yongyu Mu, Yuzhang Wu, Yuchun Fan, Chenglong Wang, Hengyu Li, Qiaozhi He, Murun Yang,  
 579 Tong Xiao, and Jingbo Zhu. Cross-layer attention sharing for large language models, 2024. URL  
 580 <https://arxiv.org/abs/2408.01890>.

581

582 Team OLMo, Pete Walsh, Luca Soldaini, Dirk Groeneveld, Kyle Lo, Shane Arora, Akshita  
 583 Bhagia, Yuling Gu, Shengyi Huang, Matt Jordan, et al. 2 olmo 2 furious. *arXiv preprint*  
 584 *arXiv:2501.00656*, 2024.

585

586 A Paszke. Pytorch: An imperative style, high-performance deep learning library. *arXiv preprint*  
 587 *arXiv:1912.01703*, 2019.

588

589 Alec Radford, Jeffrey Wu, Rewon Child, David Luan, Dario Amodei, Ilya Sutskever, et al. Language  
 590 models are unsupervised multitask learners. *OpenAI blog*, 1(8):9, 2019.

591

592 Rafael Rafailov, Archit Sharma, Eric Mitchell, Christopher D Manning, Stefano Ermon, and Chelsea  
 593 Finn. Direct preference optimization: Your language model is secretly a reward model. *Advances*  
 594 *in neural information processing systems*, 36:53728–53741, 2023.

595

596 David Raposo, Sam Ritter, Blake Richards, Timothy Lillicrap, Peter Conway Humphreys, and  
 597 Adam Santoro. Mixture-of-depths: Dynamically allocating compute in transformer-based lan-  
 598 guage models. *arXiv preprint arXiv:2404.02258*, 2024.

594 Keisuke Sakaguchi, Ronan Le Bras, Chandra Bhagavatula, and Yejin Choi. Winogrande: an adver-  
 595 sarial winograd schema challenge at scale. *Commun. ACM*, 64(9):99–106, August 2021. ISSN  
 596 0001-0782. doi: 10.1145/3474381. URL <https://doi.org/10.1145/3474381>.

597

598 Noam Shazeer. Fast transformer decoding: One write-head is all you need. *arXiv preprint*  
 599 *arXiv:1911.02150*, 2019.

600 Mingjie Sun, Xinlei Chen, J Zico Kolter, and Zhuang Liu. Massive activations in large language  
 601 models. In *First Conference on Language Modeling*, 2024. URL <https://openreview.net/forum?id=F7aAhfitX6>.

602

603 Qi Sun, Marc Pickett, Aakash Kumar Nain, and Llion Jones. Transformer layers as painters. In  
 604 *Proceedings of the AAAI Conference on Artificial Intelligence*, volume 39, pp. 25219–25227,  
 605 2025.

606

607 Hugo Touvron, Louis Martin, Kevin Stone, Peter Albert, Amjad Almahairi, Yasmine Babaei, Niko-  
 608 lay Bashlykov, Soumya Batra, Prajjwal Bhargava, Shruti Bhosale, et al. Llama 2: Open founda-  
 609 tion and fine-tuned chat models. *arXiv preprint arXiv:2307.09288*, 2023.

610

611 A Vaswani. Attention is all you need. *Advances in Neural Information Processing Systems*, 2017.

612

613 Elena Voita, David Talbot, Fedor Moiseev, Rico Sennrich, and Ivan Titov. Analyzing multi-head  
 614 self-attention: Specialized heads do the heavy lifting, the rest can be pruned. In Anna Korhonen,  
 615 David Traum, and Lluís Màrquez (eds.), *Proceedings of the 57th Annual Meeting of the Associa-  
 616 tion for Computational Linguistics*, pp. 5797–5808, Florence, Italy, July 2019. Association for  
 617 Computational Linguistics. doi: 10.18653/v1/P19-1580. URL <https://aclanthology.org/P19-1580/>.

618

619 Thomas Wolf, Lysandre Debut, Victor Sanh, Julien Chaumond, Clement Delangue, Anthony Moi,  
 620 Pierrick Cistac, Tim Rault, Rémi Louf, Morgan Funtowicz, Joe Davison, Sam Shleifer, Patrick  
 621 von Platen, Clara Ma, Yacine Jernite, Julien Plu, Canwen Xu, Teven Le Scao, Sylvain Gug-  
 622 ger, Mariama Drame, Quentin Lhoest, and Alexander M. Rush. Transformers: State-of-the-art  
 623 natural language processing. In *Proceedings of the 2020 Conference on Empirical Methods in  
 624 Natural Language Processing: System Demonstrations*, pp. 38–45, Online, October 2020. As-  
 625 sociation for Computational Linguistics. URL <https://www.aclweb.org/anthology/2020.emnlp-demos.6>.

626

627 Guangxuan Xiao, Yuandong Tian, Beidi Chen, Song Han, and Mike Lewis. Efficient streaming  
 628 language models with attention sinks. In *The Twelfth International Conference on Learning Rep-  
 629 resentations*, 2024. URL <https://openreview.net/forum?id=NG7sS51zVF>.

630

631 An Yang, Baosong Yang, Beichen Zhang, Binyuan Hui, Bo Zheng, Bowen Yu, Chengyuan Li,  
 632 Dayiheng Liu, Fei Huang, Haoran Wei, et al. Qwen2. 5 technical report. *arXiv preprint*  
*arXiv:2412.15115*, 2024.

633

634 Zhongzhi Yu, Zheng Wang, Yonggan Fu, Huihong Shi, Khalid Shaikh, and Yingyan Celine Lin. Un-  
 635 veiling and harnessing hidden attention sinks: Enhancing large language models without training  
 636 through attention calibration. In *Forty-first International Conference on Machine Learning*, 2024.  
 637 URL <https://openreview.net/forum?id=DLTjFFiuUJ>.

638

639

640

641

642

643

644

645

646

647

648 A APPENDIX  
649650 A.1 DEFINING AN ATTENTION HEAD OUTPUT  
651

652 Vaswani (2017) define an attention head output as the convex combination of value states, resulting  
653 in a  $d_v$ -dimensional vector where  $d_v = \frac{d_{\text{model}}}{h}$ ,  $d_{\text{model}}$  is the hidden size, and  $h$  is the number of heads.  
654 Other works multiply the  $d_v$ -dimensional vector by a  $\mathbb{R}^{d_v \times d_{\text{model}}}$  slice of the output projection matrix  
655 (Elhage et al., 2021). This is often called the “circuit-based” definition. In the following, we explain  
656 why this choice does not affect our intervention results.  
657

658 Given  $N$  input tokens, an attention head will multiply attention weights  $A_i \in \mathbb{R}^{N \times N}$  with value  
659 states  $V_i \in \mathbb{R}^{N \times d_v}$  so that  $Z_i = A_i V_i \in \mathbb{R}^{N \times d_k}$  for  $i = 1 \dots h$ , where  $i$  is the head index. In  
660 multi-head attention, we first concatenate  $H = [Z_1; \dots; Z_h] \in \mathbb{R}^{N \times (hd_v)}$ . Then, do an output  
661 projection

$$662 Y = H W_O \quad \text{with} \quad W_O \in \mathbb{R}^{(hd_v) \times d_{\text{model}}}$$

663 Elhage et al. (2021) partition  $W_O$  row-wise into  $h$  blocks of size  $d_v \times d_{\text{model}}$ :  
664

$$665 \quad W_O = \begin{bmatrix} W_O^{(1)} \\ W_O^{(2)} \\ \vdots \\ W_O^{(h)} \end{bmatrix}, \quad W_O^{(i)} \in \mathbb{R}^{d_v \times d_{\text{model}}} \quad (2)$$

672 Then they note that the output can be written exactly as the sum of  $h$  terms:  
673

$$674 \quad Y = \sum_{i=1}^h Z_i W_O^{(i)} \quad (3)$$

675 Elhage et al. (2021) use the above to argue that attention heads are independent saying that this is  
676 “equivalent to running heads independently, multiplying each by its own output matrix, and adding  
677 them into the residual stream.” But crucially, before we add the output of the attention module to  
678 the residual stream, we actually add up all head contributions (*i.e.*, the summation in Equation (3)).  
679 This means that  $W_O$  can implement cancellations (if, for example, two head contributions sum to  
680 zero) or other special linear combinations of heads.  
681

682 **Our choice and why it does not affect results in Section 4.3.** Because  $W_O$  mixes all heads’  
683 outputs into the shared model space, we did not want to integrate these parameters into our  
684 measurement. Thus, we define the pre-output-projection  $Z_i$  as the attention head output. Importantly,  
685 whether we choose to define  $Z_i$  or  $Z_i W_O^{(i)}$  as the  $i^{\text{th}}$  head’s output, when “zero out a head”  $Z_i$ , both  
686 will be zero.  
687

688 Table 3: **Circuit-based definition of head output.** We measure the percent of model heads that  
689 can be removed while maintaining accuracy within 1% of baseline (higher is better). For 3 different  
690 models evaluated on MMLU, using the circuit-based definition of a head output is comparable to  
691 using the original definition.  
692

693 Model	694 AWFT	695 AHON (LN)	696 Circuit-based AHON (LN)
697 Llama-3.1-8B-Instruct	698 1.01	699 <b>10.97</b>	700 9.88
701 Qwen2.5-3B	5.67	<b>7.29</b>	5.95
Qwen2.5-7B	1.25	7.54	<b>9.04</b>
Average	2.64	<b>8.60</b>	8.29

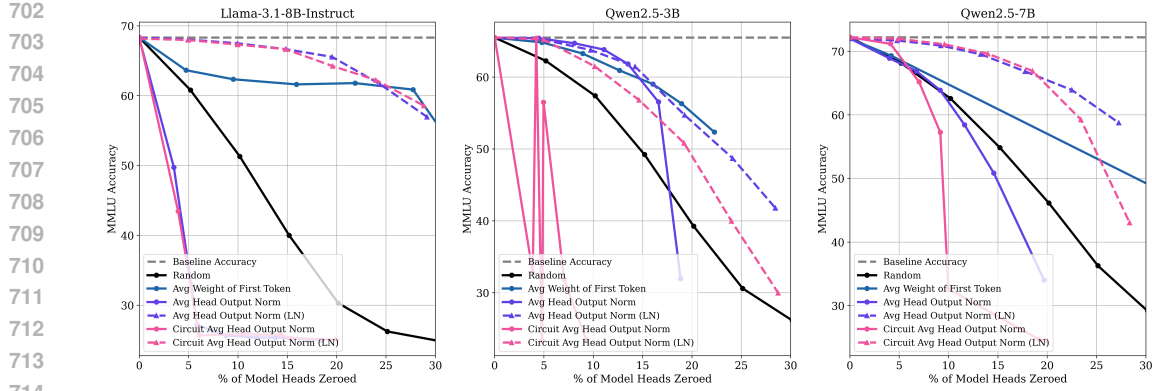


Figure 6: **Circuit-based definition of head output.** For 3 different models evaluated on MMLU, using the normalized circuit-based definition of a head output is comparable to using the original definition. Dashed lines denote layer normalized (LN) score functions.

**Implementing the circuit-based definition.** We implement the circuit-based definition of Average Head Output Norm (LN), and evaluate it on MMLU using 3 models in Figure 6. More specifically, this means that for every head of index  $i$  we measure the norms of the rows of  $Z_i W_O^{(i)} \in \mathbb{R}^{N \times d_{\text{model}}}$ , then average them to produce a score. Table 3 quantitatively shows that the percent of heads that can be zeroed using both definitions is comparable.

## A.2 ADDITIONAL NORMALIZATION STRATEGIES

In Section 3, we describe normalization by the score of other heads in the same layer. For score functions that measure a particular token in the sequence, like Last Token Head Output Norm, it is also possible to normalize by other vectors within the same head. We refer to normalization by other vectors in the same head as head normalization, or “(HN)” within this Appendix. We explored this normalization strategy with the Last Token Head Output Norm score function, but found it was always worse than the layer normalization, “(LN)”. HN is only included in App. Figures 9 to 11.

## A.3 SAMPLE INACTIVE HEADS USING SCORE FUNCTIONS

In Figure 7, we give examples of attention heads that are identified by each unnormalized score function, by using threshold-based rules of Table 1. To keep each attention weights matrix small, we use a random, short 50 token sequence from FineWeb-Edu and execute a forward pass on Qwen2.5-7B and OLMo-2-1124-7B. In Figure 8, we show how the normalized AHON (LN) score function can capture distinct kinds of heads. For example, the first head has a first token sink, the second head has two sinks, and the third head has a second token sink. AHON (LN) is able to identify all three as inactive.

As a summary of the kind of head that each score function is meant to capture, we provide a short explanation for each:

- Avg Weight of First Token (AWFT): When attention concentrates on first token
- Avg Entropy of Query Distributions (AEQD): When attention concentrates on a few tokens
- First Token Value Vector Norm (FTVVN): When first value vector is near-zero
- Avg Value Vector Norm (AVVN): When most value vectors are near-zero
- Last Token Head Output Norm (LTHON): When last head output token near-zero
- Avg Head Output Norm (AHON): When most head output tokens are near-zero

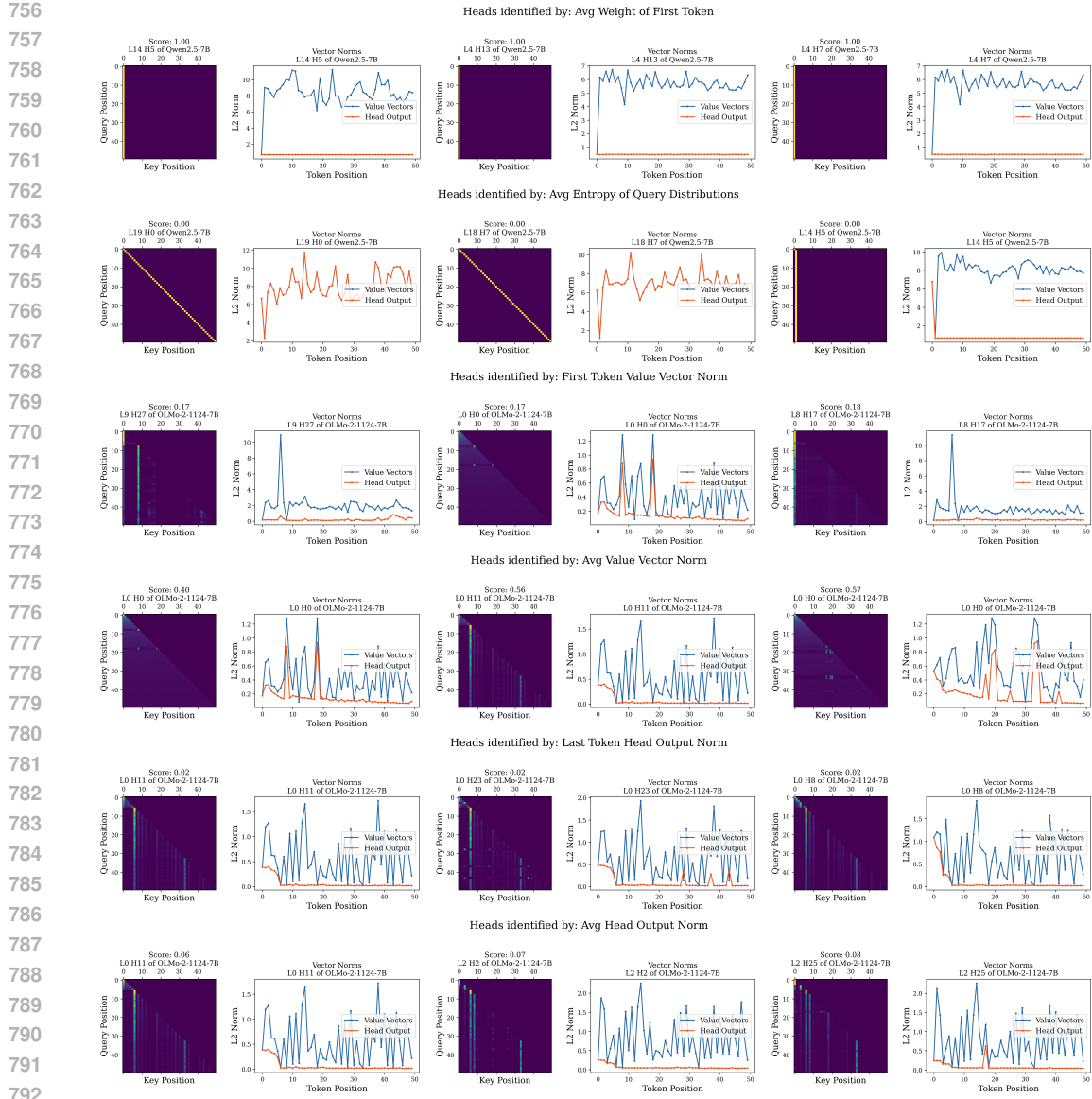


**Figure 7: Sample Attention Heads for 6 Unnormalized Score Functions.** In each row, we plot 3 sample attention heads for each score function in Table 1. To the right of each attention weights matrix, we plot the  $\ell_2$ -norm of Value Vectors and Head Outputs. We also include the layer index and head index of each attention head above each plot. Lower scores are better for all score functions other than AWFT. Note the variety of heads that are identified by each score function.

#### A.4 FULL RESULTS OF SECTION 4.3

In Section 4.3 Figure 4, we present intervention results for 3 models. Results for all 14 models are presented in Figure 9.

##### A.4.1 ADDITIONAL DATASETS

We also run the same experiments and analysis on the PIQA (0-shot) (Bisk et al., 2020) and Wino-Grande (5-shot) Sakaguchi et al. (2021) datasets. Plots on how accuracy degrades with different percent of model heads zeroed can be found in Figures 10 and 11. The quantitative analysis, where we measure the maximum proportion of heads that we can zero while maintaining accuracy to within

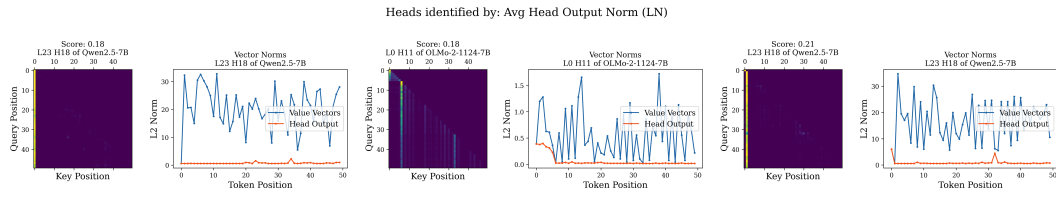


Figure 8: **Sample Attention Heads using Avg Head Output Norm (LN).** We plot 3 sample attention heads for AHON (LN), the best score function by AUC (See Figure 3). To the right of each attention weights matrix, we plot the  $\ell_2$ -norm of Value Vectors and Head Outputs. Note that the first head has a first token sink, the second head has two sinks, and the third head has a second token sink. AHON (LN) is able to capture all three distinct heads.

1% of the original model can be found in Tables 4 and 5. On PIQA, our score functions show that more than 21% of attention heads can be zeroed while keeping average accuracy within 1% of the original model. On WinoGrande, more than 14% of attention heads can be zeroed while keeping average accuracy within 1% of the original model. Thus, our claim in the main body of the paper is a conservative estimate of inactive heads. In all cases, our score functions can identify more heads than Avg Weight of First Token (AWFT).

Table 4: **PIQA Benchmark: On average, more than 21% of attention heads can be zeroed while keeping average accuracy within 1% of the original model.** For every model, we calculate the highest percentage of heads that can be zeroed using Average Weight of First Token (AWFT), and compare to our score functions (*i.e.*, all score functions excluding AWFT). Higher is better. The overall best score function is also shown. We are able to identify and verify more inactive heads than previously possible with AWFT.

Model	% of Heads Zeroed		Best Score Function
	AWFT	Ours	
Llama-3.2-3B	21.76	17.37 (-4.39)	Avg Weight of First Token
Llama-3.2-3B-Instruct	15.32	25.78 (+10.46)	Avg Head Output Norm (LN)
Llama-3.1-8B	0.00	17.85 (+17.85)	First Token Value Vector Norm (LN)
Llama-3.1-8B-Instruct	31.30	25.39 (-5.91)	Avg Weight of First Token
OLMo-2-1124-7B	20.74	22.70 (+1.97)	Avg Head Output Norm (LN)
OLMo-2-1124-7B-SFT	1.87	20.12 (+18.26)	Last Token Head Output Norm (LN)
OLMo-2-1124-7B-DPO	2.93	15.87 (+12.94)	First Token Value Vector Norm (LN)
OLMo-2-1124-7B-Instruct	2.54	26.83 (+24.30)	Avg Head Output Norm (LN)
Qwen2.5-0.5B	0.00	18.36 (+18.36)	Avg Head Output Norm (LN)
Qwen2.5-1.5B	24.33	21.32 (-3.01)	Avg Weight of First Token
Qwen2.5-3B	16.51	21.42 (+4.91)	Avg Head Output Norm
Qwen2.5-7B	0.00	28.66 (+28.66)	First Token Value Vector Norm
Qwen2.5-7B-Instruct	2.84	11.45 (+8.61)	Avg Head Output Norm (LN)
Qwen2.5-14B	0.00	26.12 (+26.12)	First Token Value Vector Norm (LN)
Average	10.01	21.38 (+11.37)	-

All models and score function evaluations can be found in Figure 9.

### A.5 INACTIVE HEAD DISTRIBUTIONS BY LAYER

Using OLMo-2-1124-7B-Instruct and 3 datasets (MMLU, PIQA (Bisk et al., 2020), and WinoGrande (Sakaguchi et al., 2021)), we plot the percent of inactive heads per layer in Figure 12. We consider two score functions, Average Weight of First Token (Gu et al., 2025) and Average Head Output Norm (LN) (the best performing method in Section 4.3). We choose thresholds such that  $\sim 15\%$  of heads are identified as potentially inactive. Specifically, for OLMo-2-1124-7B-Instruct,

864  
 865 **Table 5: WinoGrande Benchmark: On average, more than 14% of attention heads can be**  
 866 **zeroed while keeping average accuracy within 1% of the original model.** For every model, we  
 867 calculate the highest percentage of heads that can be zeroed using Average Weight of First Token  
 868 (AWFT), and compare to our score functions (*i.e.*, all score functions excluding AWFT). Higher is  
 869 better. The overall best score function is also shown. We are able to identify and verify more inactive  
 870 heads than previously possible with AWFT.

871 Model	872 % of Heads Zeroed		873 Best Score Function
	874 AWFT	875 Ours	
Llama-3.2-3B	9.11	11.64 (+2.53)	Avg Head Output Norm (LN)
Llama-3.2-3B-Instruct	5.57	20.37 (+14.79)	Avg Head Output Norm (LN)
Llama-3.1-8B	6.86	17.08 (+10.22)	Avg Head Output Norm (LN)
Llama-3.1-8B-Instruct	12.44	11.89 (-0.55)	Avg Weight of First Token
OLMo-2-1124-7B	15.39	16.12 (+0.73)	Avg Head Output Norm (LN)
OLMo-2-1124-7B-SFT	2.32	19.00 (+16.68)	Avg Head Output Norm (LN)
OLMo-2-1124-7B-DPO	2.79	16.94 (+14.15)	Avg Head Output Norm (LN)
OLMo-2-1124-7B-Instruct	3.02	20.91 (+17.89)	Last Token Head Output Norm (LN)
Qwen2.5-0.5B	6.49	11.35 (+4.86)	Avg Head Output Norm (LN)
Qwen2.5-1.5B	7.49	12.68 (+5.18)	First Token Value Vector Norm
Qwen2.5-3B	5.73	10.32 (+4.60)	First Token Value Vector Norm
Qwen2.5-7B	6.60	15.69 (+9.10)	First Token Value Vector Norm (LN)
Qwen2.5-7B-Instruct	2.00	8.03 (+6.03)	Avg Value Vector Norm (LN)
Qwen2.5-14B	10.80	10.25 (-0.55)	Avg Weight of First Token
Average	6.90	14.45 (+7.55)	-

889 we use a AWFT threshold  $\tau$  of 0.077 for MMLU, 0.265 for PIQA, and 0.109 for WinoGrande. We  
 890 use AHON (LN) threshold of 0.457 for MMLU, 0.435 for PIQA, and 0.473 for WinoGrande. Note  
 891 that thresholds for our normalized score function are more similar, indicating their generality across  
 892 datasets.

893 When using Average Weight to First Token as the score function (Figure 12, Left), there are sig-  
 894 nificant differences between MMLU and PIQA: On MMLU, inactive heads tend to occur in later  
 895 layers, averaging above  $\sim 60\%$  of inactive heads in layer index 23. But for PIQA, inactive heads  
 896 tend to occur in early layers, averaging above  $\sim 50\%$  of inactive heads in layer index 3. There is  
 897 less variance among datasets when using Average Head Output Norm (LN) as the score function  
 898 (Figure 12, Right), demonstrating the consistency of our score function across data distributions.

## 900 A.6 MULTIPLE FORWARD PASS ANALYSIS

901 The main body of the paper focuses on analyzing a single forward pass because that is how log-  
 902 likelihood evaluations of MMLU, PIQA, WinoGrande and other MC benchmarks are performed. To  
 903 explore how heads may change from inactive to active, based on increasing context, we choose 3  
 904 FineWeb-Edu train sequences of at least 512 OLMo-2 tokens in length:

- 905 • Seq 0 ID: urn:uuid:0d8a309d-25c5-405d-a08a-c11239f0d717. Category: Literary com-  
 906 mentsary.
- 907 • Seq 1 ID: urn:uuid:316c7af5-14e1-4d0b-9576-753e17ef2cc5. Category: Popular Science  
 908 or Journalism.
- 909 • Seq 2 ID: urn:uuid:c337bcd8-6aa1-4f2d-8c48-b916442ebbee. Category: Educational arti-  
 910 cle on software licensing.

911 We choose to evaluate inactive heads of OLMo-2-1124-7B-Instruct as each of these sequences grows  
 912 in Figure 13. We analyze AWFT and AHON (LN) score functions because AWFT is prior work,  
 913 and AHON (LN) is the best score function we discover in Section 4.3. As expected, AWFT presents  
 914 decaying curves where the model has fewer inactive heads as sequence length increases. As se-  
 915 quences increase in length, each query has more potential tokens it can attend to, making it less

likely that the first token receives disproportionate attention. Additionally, as can be seen in Figure 20 and Appendix A.3, OLMo-2 models tend to use additional sink tokens (not just the first token). In contrast, measuring AHON (LN) inactive heads as sequence length increases, we observe noisy measurements of inactive head proportions in short sequences that converge as each sequence gets sufficiently long. In measuring both AWFT and AHON (LN) inactive heads, it is clear that inactivity is context-dependent.

We are also interested in where changing attention heads are located. We examine inactive head masks for AWFT and AHON (LN) in Figures 14 and 15. Every matrix cell indicates a particular attention head, and we color yellow any head that is identified as inactive. Unlike AWFT score function measurements, AHON (LN) inactive heads are more spread out throughout the model. We also observe the same phenomenon in Appendix A.5 Figure 12.

### A.7 SCORE DISTRIBUTIONS ON MMLU

All score function distributions, from MMLU, can be found in Figure 16.

### A.8 FULL RESULTS OF SECTION 4.4 WASSERSTEIN DISTANCES

All Wasserstein distance matrices, for all score functions, can be found in Figure 17.

### A.9 SCORE DISTRIBUTIONS COMPARISON: FINEWEB-EDU VS. MMLU

In Figure 18, we show how the distribution of Avg Weight of First Token scores change when the input dataset changes. Qwen2.5-7B has a small fraction of heads that exceed 0.8 average attention to the first token on FineWeb-Edu, but on MMLU there are essentially none. One explanation is the token sequence length which, for 5-shot MMLU, tend to be approximately 3000 tokens long. In contrast, the FineWeb-Edu sequences we use are randomly truncated to be between 30 and 3000 tokens.

### A.10 ATTENTION SINKS AND VALUE-STATE DRAINS

Sample attention sink patterns and value-state drains can be found in Figure 19.

### A.11 REDUNDANCY OF ATTENTION PATTERNS

Numerous works have noted the prevalence of redundant attention patterns across attention heads, even from different layers Xiao et al. (2024); Mu et al. (2024); Guo et al. (2024a); Liu et al. (2023); Ge et al. (2024), and attention sinks make up part of those patterns. In Figure 20, we observe the same phenomena in recent pretrained LLMs. We plot attention matrices from the last 8 layers of five models. The chosen head indices are simply ordered sequentially. Not only are attention patterns similar among heads of every model, different models have different sink token behaviors. Llama-2-7b-hf uses two sinks and divides weight between them. Llama-3.1-8B uses the first token as a sink. OLMo-2-1124-7B, like Llama-2-7b-hf, uses two sink tokens, but the second intermediate sink is at a different position than that of Llama-2-7b-hf. Qwen2.5-7B tends to use the *second* token as a sink, while Qwen2.5-14B uses the first token. We exclude Llama-3.2-3B from Figure 20 because it presents similar attention patterns to Llama-3.1-8B.

For every model in Figure 20, we also show the top 2 principal components across all attention matrices (of which there are  $N_{\text{layer}} \times N_{\text{heads}}$ ). It is surprising to see a few principal components capturing more than half of the observed variance of attention matrices, for all models.

The input to all models in Figure 20 is from MMLU’s `high_school_computer_science`, `dev` split, index 2. The input text is in the same format used by `lm-evaluation-harness` (Gao et al., 2024):

The following are multiple choice questions (with answers) about high school computer science.

What is the output of "abc"[::-1] in Python 3?

```

972 A. Error
973 B. abc
974 C. cba
975 D. c
976 Answer:
977

```

### A.12 ON LM-EVALUATION-HARNESS EVALUATIONS

For reliable and complete evaluations, use `batch_size='auto'` in `lm-evaluation-harness`. It not only finds an optimal batch size for your hardware to prevent memory errors but also mitigates the issue where an entire batch may be skipped because one sample cannot fit on the GPU.

### A.13 PYTORCH IMPLEMENTATION OF AVG HEAD OUTPUT NORM (LN) AND AVG WEIGHT TO FIRST TOKEN

We provide sample PyTorch code (Paszke, 2019), for Avg Head Output Norm (LN) and Avg Weight to First Token, that can be integrated into a self-attention module’s forward pass. When using `lm-evaluation-harness` (Gao et al., 2024) to evaluate pretrained models, additional steps must be taken to ignore padding tokens during log likelihood evaluations (on MC datasets).

All score functions are implemented within the self-attention module and take as input the following tensors: attention weights of size  $(B, N_{\text{head}}, S, S)$ , value states of size  $(B, N_{\text{head}}, S, d_v)$ , and a float threshold.  $B$  denotes the batch size,  $S$  denotes the sequence length,  $N_{\text{head}}$  denotes the number of attention heads, and  $d_v$  is the dimension of the value states. As output, both implementations return a boolean mask of dormant heads of size  $(B, N_{\text{head}})$  and attention outputs of size  $(B, N_{\text{head}}, S, d_v)$ . In the dormant mask, an entry is True if the head is declared dormant, and False otherwise. Note that models that use grouped-query attention (GQA) (Ainslie et al., 2023) or multi-query attention (MQA) (Shazeer, 2019) still construct tensors of these sizes, so the specific kind of multi-head attention is not relevant.

Listing 1: Avg Weight to First Token in PyTorch

```

1 def awft_dormant_mask(attn_weights, value_states, threshold):
2     avg_weight = attn_weights.mean(dim=-2) # (B, N_head, S)
3     first_token_avg_weight = avg_weight[:, :, 0] # (B, N_head)
4     dormant_mask = first_token_avg_weight > threshold # (B, N_head)
5
6     # Model intervention: set dormant head outputs to zero
7     attn_output = torch.matmul(attn_weights, value_states)
8     attn_output[dormant_mask] = 0
9     return attn_output, dormant_mask

```

Listing 2: Avg Head Output Norm (LN) in PyTorch, following Equation (1)

```

1 def ahon_ln_dormant_mask(attn_weights, value_states, threshold):
2     attn_output = torch.matmul(attn_weights, value_states)
3     norm_per_token = attn_output.norm(dim=-1) # (B, N_head, S)
4     avg_norm_per_head = norm_per_token.mean(dim=-1) # (B, N_head)
5
6     # compute average across all heads in layer
7     layer_context = avg_norm_per_head.mean(dim=1) # (B, )
8     rel_avg_norm_per_head = (avg_norm_per_head / layer_context[:, None])
9     # (B, N_head)
10    dormant_mask = rel_avg_norm_per_head < threshold # (B, N_head)
11
12    # Model intervention: set dormant head outputs to zero
13    attn_output[dormant_mask] = 0
14    return attn_output, dormant_mask

```

1026 A.14 ADDITIONAL MODEL AND DATASET INFORMATION  
1027

1028 **Model details.** Model inference is done in the original data type of the saved weights  
1029 using `AutoModelForCausalLM.from_pretrained(..., torch.dtype="auto")`, ex-  
1030 cept for OLMo-2 models, where we use `float16`. All models are downloaded using Hugging Face  
1031 (HF) `transformers` (Wolf et al., 2020). Parameter counts and release dates are shown in Table 6.

Model Name	Params	Heads Per Layer	Num Layers	Total Heads	Release Date
Llama-3.1 8B	8.03B	32	32	1024	Jul 2024
Llama-3.2-3B	3.21B	24	28	672	Sep 2024
OLMo-2-1124-7B	7.3B	32	32	1024	Nov 2024
Qwen2.5-7B	7.62B	28	28	784	Feb 2025
Qwen2.5-14B	14.8B	40	48	1920	Feb 2025

1040 Table 6: Additional model information of pretrained LLMs used in this work.  
1041

1042 **Dataset details.** The test split of the MMLU benchmark contains 14,042 multiple-choice (MC)  
1043 questions spanning 57 tasks including mathematics, US history, computer science, law, and more.  
1044 Each question has 4 answer choices.

1045 We also use PIQA (Bisk et al., 2020) and WinoGrande (Sakaguchi et al., 2021), but only in Ap-  
1046 pendix A.4 to reduce clutter in the main body. PIQA is a MC benchmark dataset of physical com-  
1047 monsense questions where each question has 2 answer choices. WinoGrande is a MC benchmark  
1048 dataset of pronoun resolution problems where each problem has 2 answer choices.  
1049

1050 A.15 PRACTICAL IMPLICATIONS AND LIMITATIONS  
1051

1052 **Architectures.** We think there is evidence that different problems require different fractions of  
1053 model parameters to solve (Raposo et al., 2024; Lin et al., 2017). Our experiments provide concrete  
1054 evidence that this occurs in self-attention, and we think sparsity can be beneficial for designing  
1055 architectures like MoEs but for attention modules. We may not need to have all heads in memory if  
1056 only a subset will be used. A router could potentially be developed to select the appropriate heads.  
1057 Our work provides necessary background on inactive attention heads so that future work can develop  
1058 new architectures for this problem.  
1059

1060 **Efficiency** It should be possible to dynamically prune different heads on-the-fly whenever we  
1061 identify a head as inactive. But it is unknown whether the overhead in identifying these heads  
1062 (by computing scores) will make inference so slow that the compute savings are not worth it. In  
1063 particular, our best score function (AHON (LN)) has the issue that it requires computing the head  
1064 output itself, making it impossible to save compute when “skipping” a head. However, future work  
1065 may discover a more proper score function that would allow for compute saving. For example,  
1066 Lin et al. (2017) showed that image classifiers could be dynamically pruned at runtime, for each  
1067 individual input. Another potential direction is KV cache compression: specifically, not storing K/V  
1068 for heads that are inactive. Our work also opens up new directions for investigation like finetuning  
1069 inactive heads.

1070 **Limitations.** We focus on analyzing a single forward pass because that is how log-likelihood  
1071 evaluations of MMLU, PIQA, WinoGrande and other MC benchmarks are performed. Analyzing  
1072 generation is complex because zeroing out a single incorrectly identified head can ruin the rest of  
1073 the generated sequence (*i.e.*, more opportunities for failure). For example, if we zero out too many  
1074 heads, we could sample a token representing a different language. Analyzing generation is a natural  
1075 next step, as it is used for more practical use-cases.

1076 A.16 LLM USAGE  
1077

1078 LLMs were used to aid or polish writing. Gemini 2.5 Pro and ChatGPT were used with prompts like  
1079 “revise this sentence”.

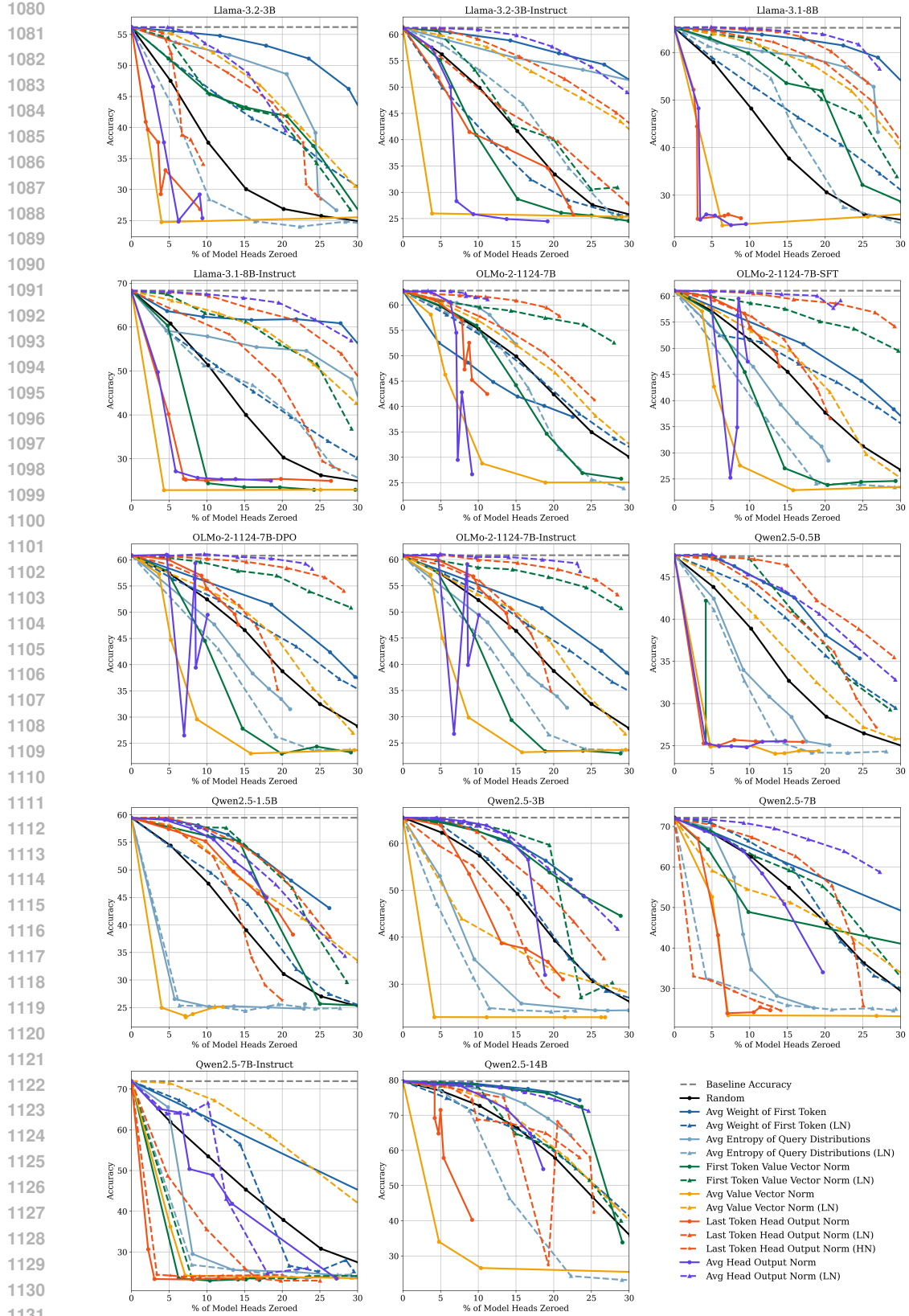
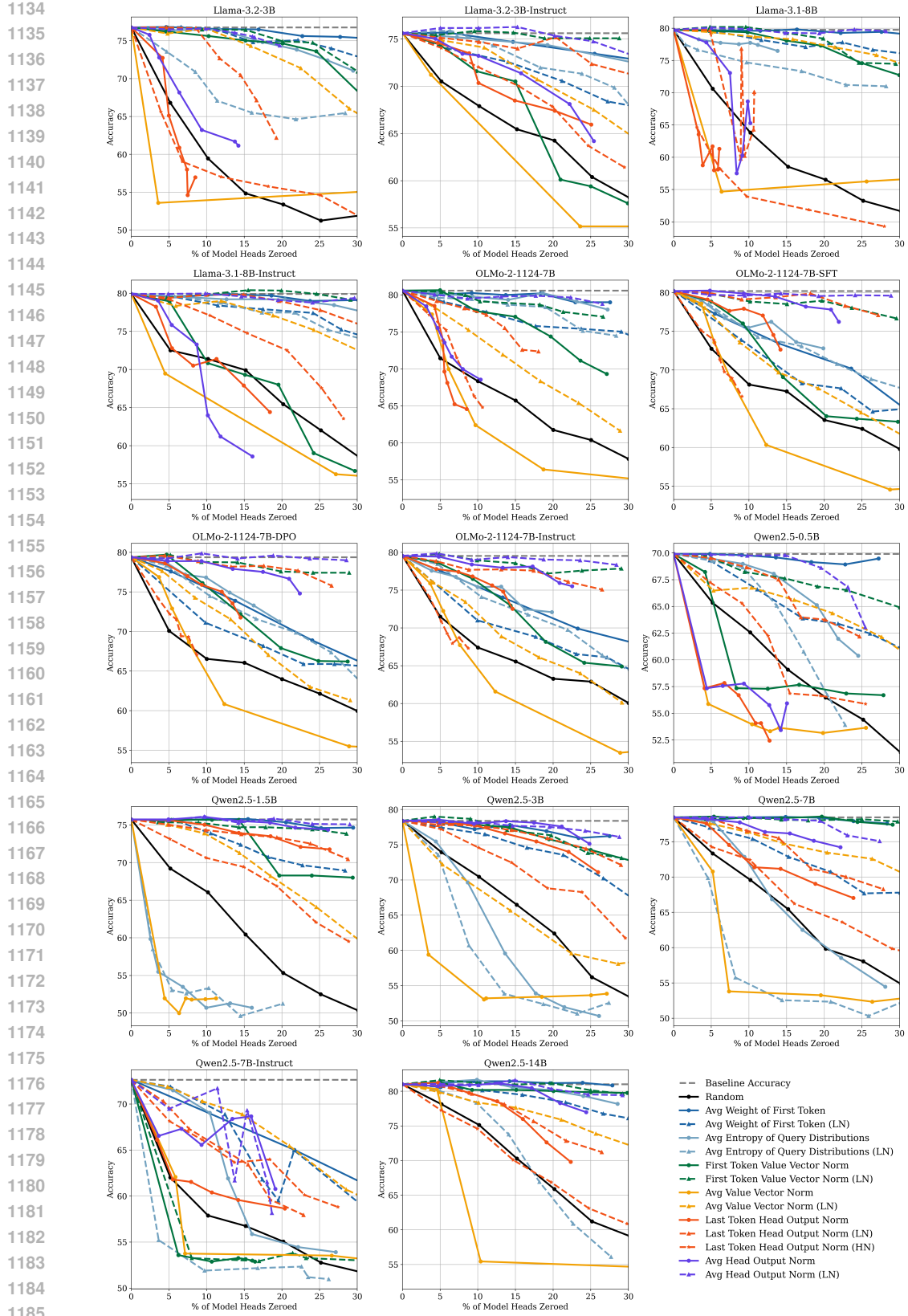
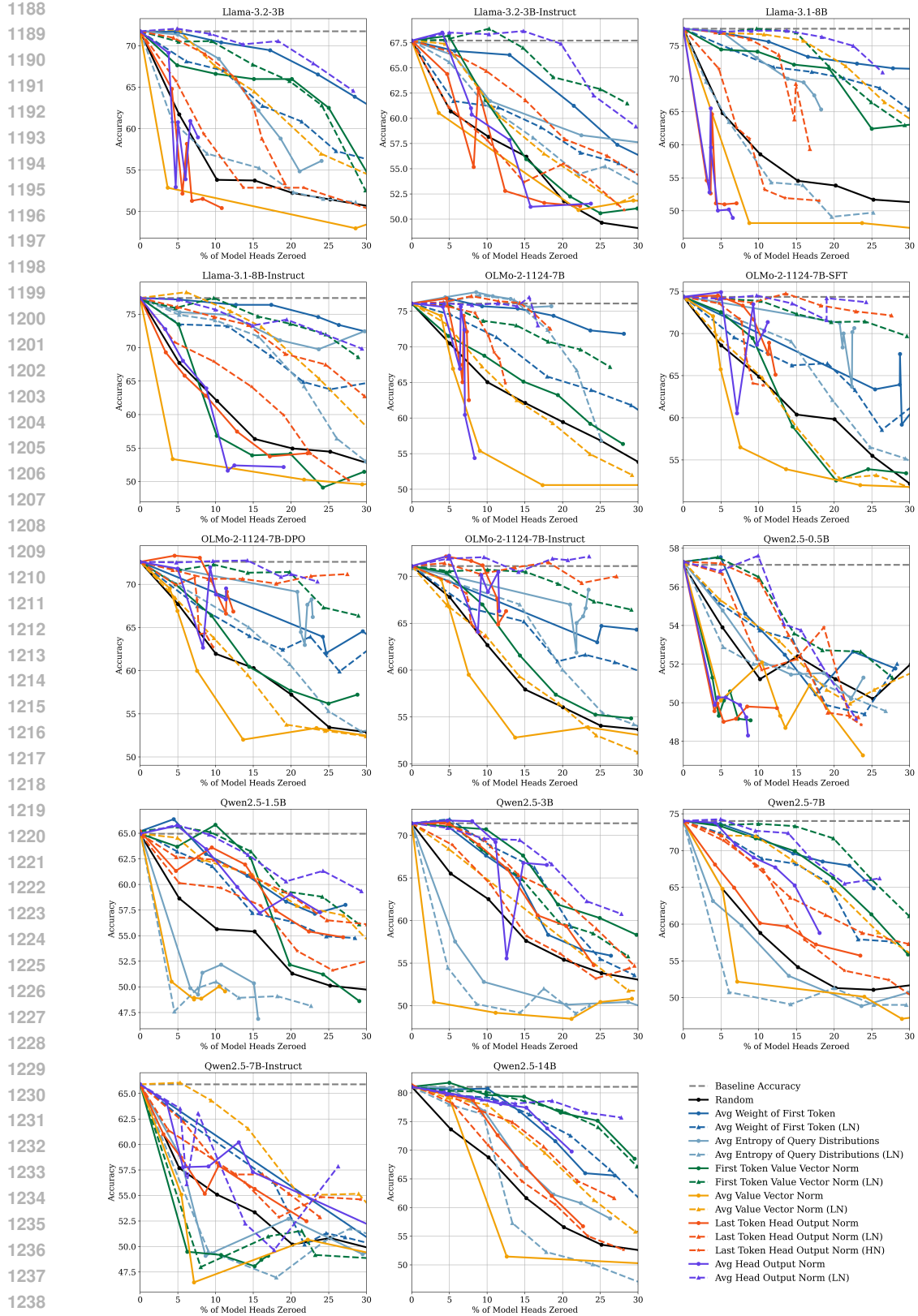


Figure 9: **Complete MMLU Results of Section 4.3.** For 14 models, we consider 13 scoring functions, and evaluate each at 7 distinct thresholds  $\tau$  for each.





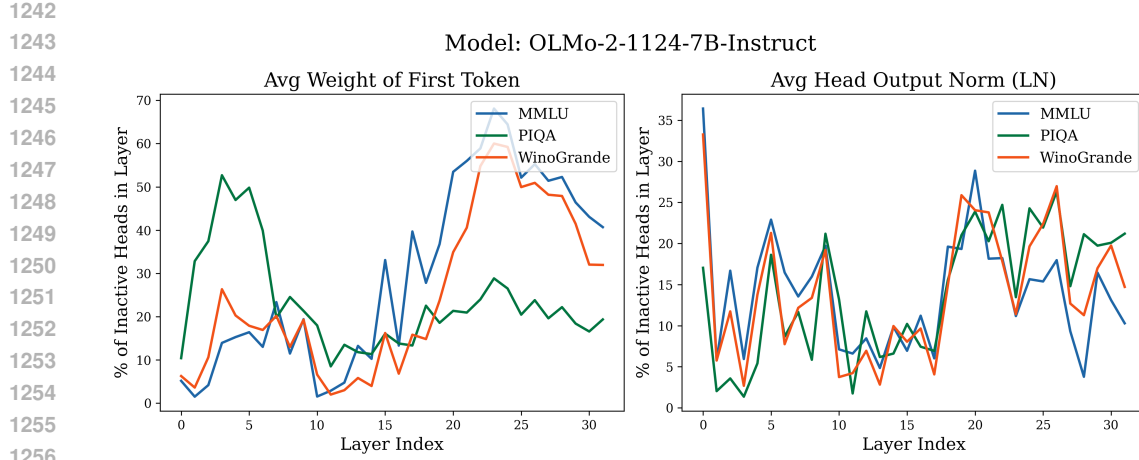


Figure 12: **Inactive Head Distribution by Layer.** For OLMo-2-1124-7B-Instruct, as for other models, the percent of heads inactive per layer varies based on the data distribution (MMLU vs. PIQA vs. WinoGrande) when using Average Weight to First Token. There is less variance among datasets when using Average Head Output Norm (LN) as the score function.

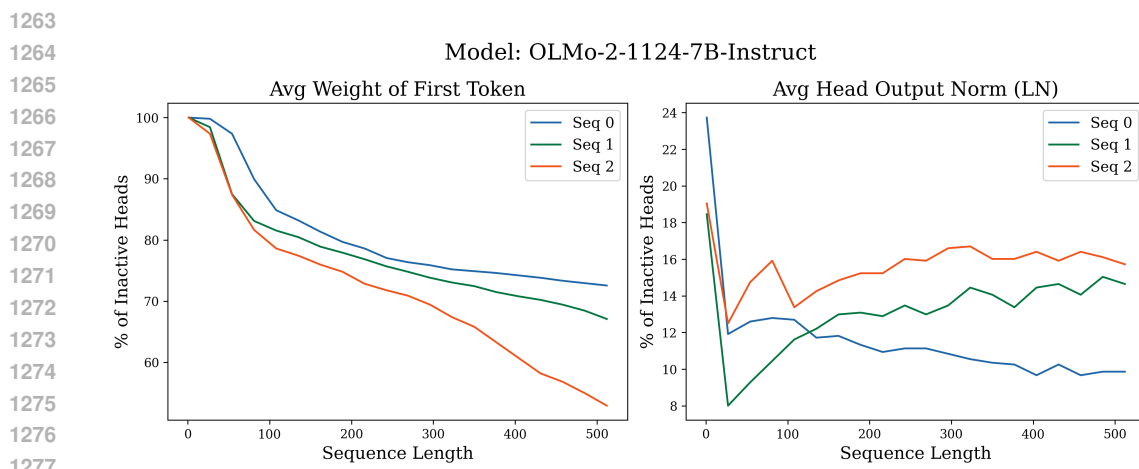


Figure 13: **Inactive Heads as Sequence Length Changes.** For OLMo-2-1124-7B-Instruct, we consider 3 FineWeb-Edu sequences, and evaluate the percent of inactive heads in the model as the sequence length increases. We compare AWFT ( $\tau = 0.077$ ) and AHON (LN) ( $\tau = 0.457$ ) score functions.

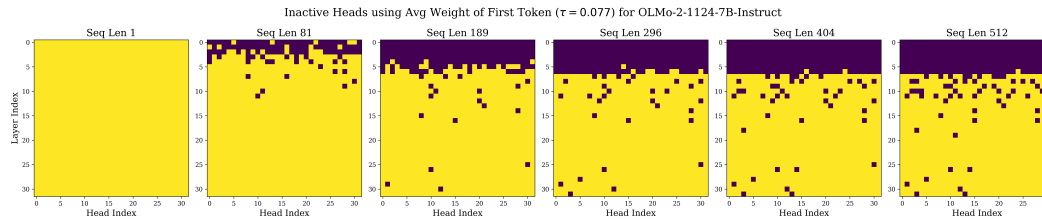
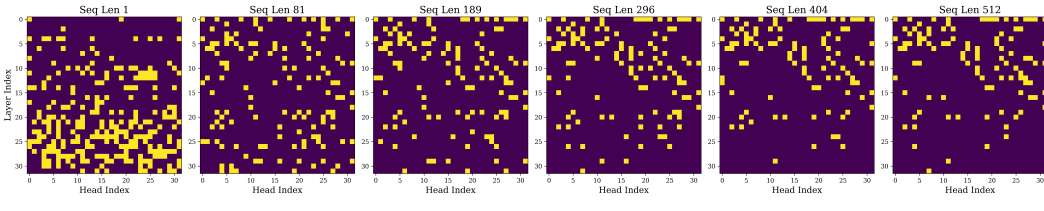
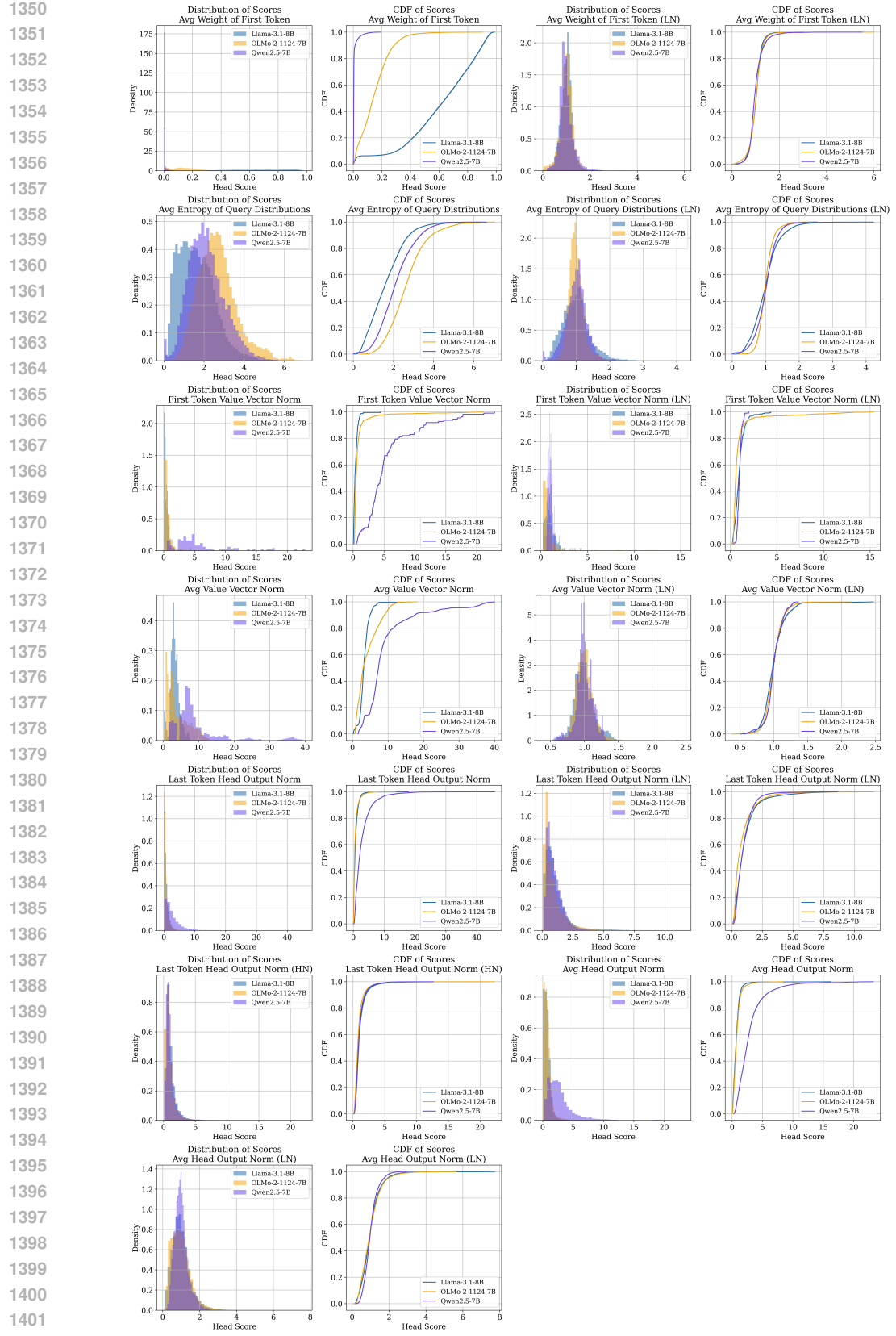
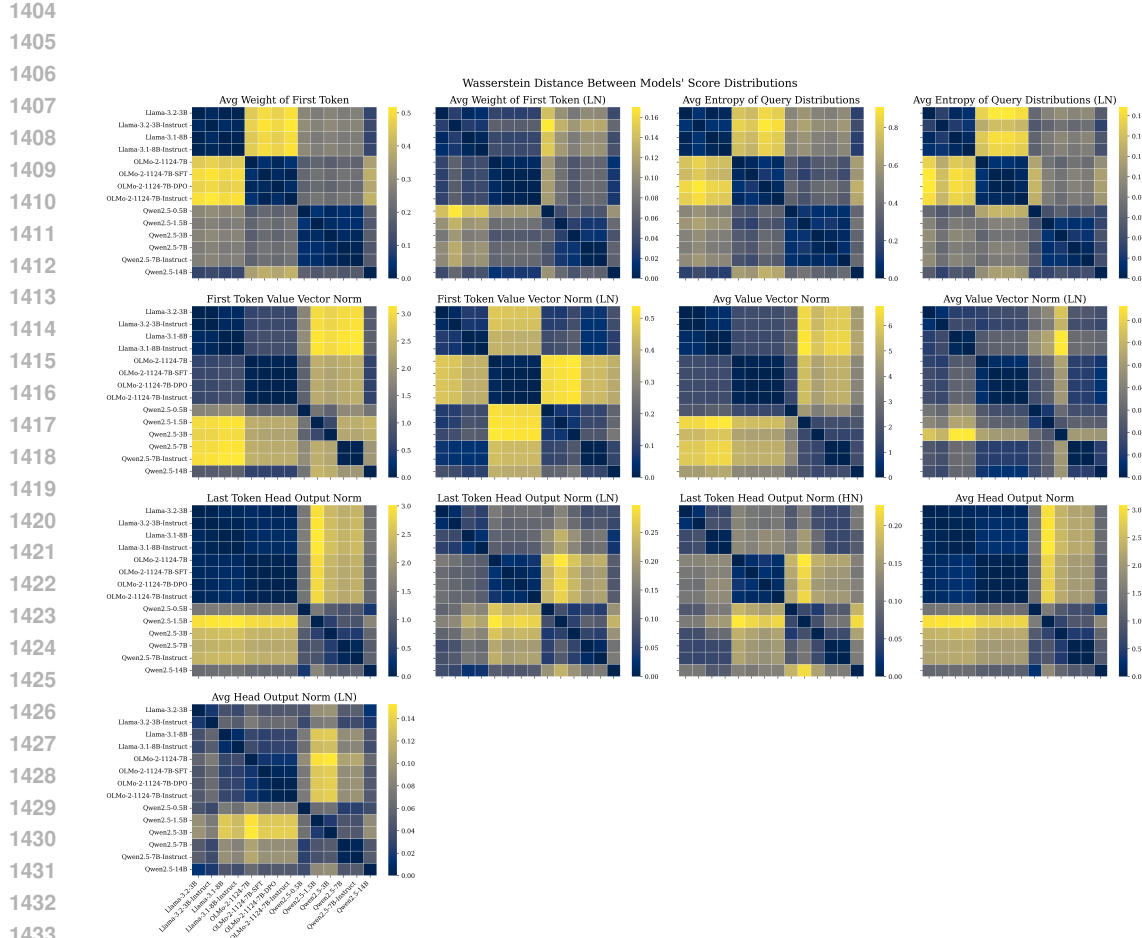


Figure 14: **Inactive Heads as Sequence Length Changes.** For OLMo-2-1124-7B-Instruct, we plot an inactive head mask for increasing sequence lengths of “Seq 0” from Figure 13. Yellow indicates an inactive head, as identified by AWFT score function.

1296  
 1297  
 1298  
 1299  
 1300  
 1301  
 1302  
 1303  
 1304  
 1305  
 1306  
 1307  
 1308  
 1309  
 1310  
 1311  
 1312  
 1313  
 1314  
 1315  
 1316  
 1317  
 1318       Inactive Heads using Avg Head Output Norm (LN) ( $\tau = 0.457$ ) for OLMo-2-1124-7B-Instruct  
 1319         
 1320  
 1321  
 1322  
 1323  
 1324  
 1325  
 1326       Figure 15: **Inactive Heads as Sequence Length Changes.** For OLMo-2-1124-7B-Instruct, we plot  
 1327       an inactive head mask for increasing sequence lengths of “Seq 0” from Figure 13. Yellow indicates  
 1328       an inactive head, as identified by AHON (LN) score function.  
 1329  
 1330  
 1331  
 1332  
 1333  
 1334  
 1335  
 1336  
 1337  
 1338  
 1339  
 1340  
 1341  
 1342  
 1343  
 1344  
 1345  
 1346  
 1347  
 1348  
 1349



**Figure 16: Head Score Distributions on MMLU.** For 13 scoring functions, we plot a density distribution and a CDF of head scores. We only show scores for Llama-3.1-8B, OLMo-2-1124-7B, and Qwen2.5-7B for brevity.



**Figure 17: Wasserstein Distance of Head Score Distributions between Models.** For each of 13 score functions, we plot a matrix of Wasserstein distances between score distributions of different models.

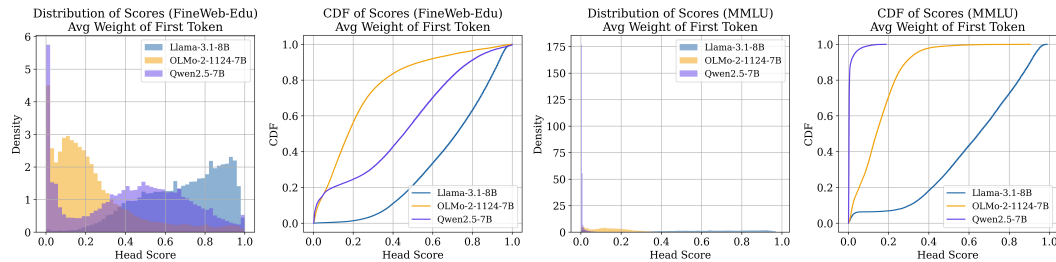


**Figure 18: Distribution of Avg Weight of First Token Scores changes when the input distribution changes.** Using the same 3 models, we find that the distribution of Avg Weight of First Token scores varies significantly when using input sequences from MMLU (right) instead of FineWeb-Edu (left).

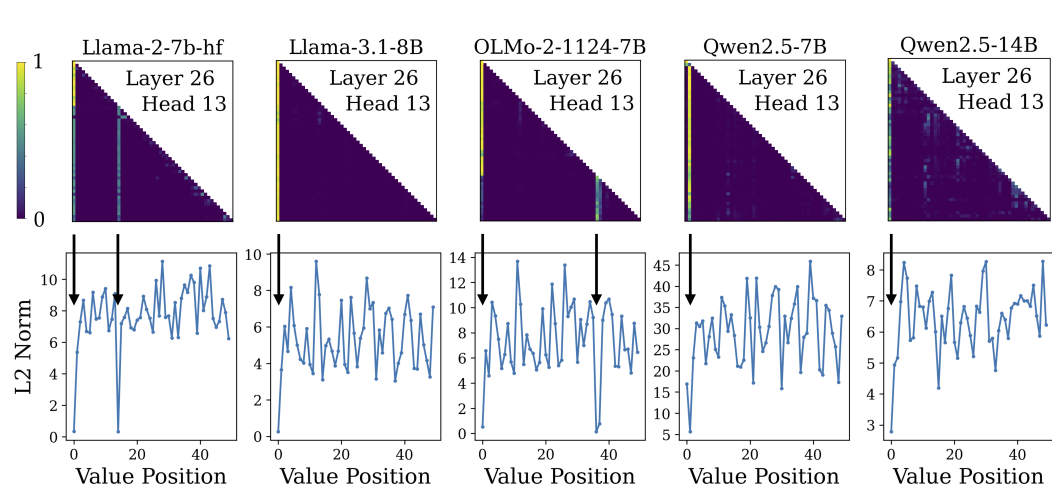
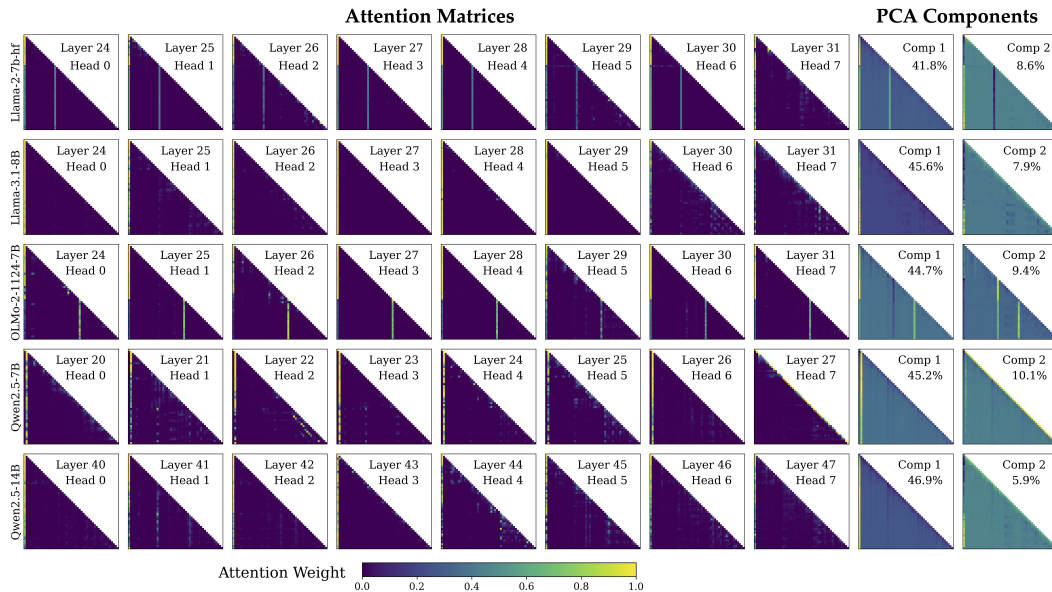


Figure 19: **Attention sink tokens have the smallest value vector norms.** For different models, we input the same question from MMLU. In the first row, we plot the attention weights for an arbitrary head (Layer 26, Head 13) across all models. In the second row, we plot the  $\ell_2$ -norm of the value vector at every position.



**Figure 20: PCA of Attention Matrices.** Attention patterns from different heads appear homogeneous and dominated by attention sinks. We input the same multiple-choice question from MMLU into Llama-2-7b-hf, Llama-3.1-8B, OLMo-2-1124-7B, Qwen2.5-7B, and Qwen2.5-14B then visualize the attention matrices. Each model row displays a sample of eight attention matrices from the last eight layers, followed by the top-2 principal components of all attention matrices, with the explained variance of each component displayed. The top-2 principal components display bright columns of attention sinks while capturing  $\geq 50\%$  of the variance. “L26 H2” denotes the attention head at index 2 of layer 26.